HYDROGEOCHEMICAL AND WATER QUALITY ASSESSMENT IN KAYELEKERA, NORTHERN MALAWI

MSc. (APPLIED CHEMISTRY) THESIS

By

Jonathan Christine Kachusa Chirwa

B.Ed. (Science) - University of Malawi

Submitted to the Department of Chemistry, Faculty of Science, in partial fulfilment of the requirements for the degree of Master of Science (Applied Chemistry)

University of Malawi

September, 2023

DECLARATION

This thesis is my own original work, and it has not been submitted to any other institution for similar purposes. Acknowledgments have been duly made where other people's work has been used. I bear the responsibility of this paper.

JONATHAN CHRISTINE KACHUSA CHIRWA

_____

Name

_____

Signature

_____

Date

CERTIFICATE OF APPROVAL

The undersigned certify that this thesis represents the student's work and has been submitted with our approval.

Signature: _____ Date: _____

Monjerezi. M., PhD (Associate Professor)

Main supervisor

Signature: _____Date: _____

Sajidu S.M.I., PhD (Professor)

Member, Supervisory Committee

Signature: _____Date: _____

Head, Department of Chemistry

DEDICATION

To my beloved daughter, Annes Msimbi Kachusa Chirwa, my mother, Annes Station Chirwa and my wife Alinafe Scholastica Chirwa. You made it all successful!

ACKNOWLEDGMENTS

My heartfelt appreciation goes to my supervisors Dr Maurice Monjerezi and Professor Samson Sajidu for their guidance, encouragement, cordial relationship, and unreserved direction throughout the writing of the thesis. I am thankful for Dr. Monjerezi for his scientific advice, critical analysis, and comments throughout the research work. Prof. Sajidu, for his extraordinary commitment, patience, and constructive comments throughout my research work.

I would like to express my sincere gratitude to the Government of Malawi and University of Malawi for giving me an opportunity to pursue my Master of Science and for the financial support towards my research, respectively. I would also like to extend my gratitude to Mr. John Mwenelupembe and Mr. Baxter Chimlambe for their unceasing support. My colleagues William Munthali, Misheck Munyimbiri, and Lyson Kanyika at Paladin Africa, you offered great support during fieldwork and sampling. I am grateful to Joel Njewa and Joseph Kanthumba for their friendship in the time of the study at the University of Malawi and to all 2017 Chemistry postgraduates. Finally, I wish to acknowledge the support and encouragement given by my mother Mrs. Annes Kachusa Chirwa which played an important role in inspiring me to complete this work. I say, “God bless you”.

ABSTRACT

Kayelekera communities depend on rivers as main source of water supply for industrial, domestic, and agricultural use. In this study, samples were collected in both rainy and dry season followed by an assessment on the state of water quality and hydro-geochemical processes controlling river water chemistry using statistical and geochemical modelling methods in Kayelekera. Hierarchical Cluster Analysis classified water samples into three distinct clusters (C1-C3) in both seasons. One - way ANOVA ($p<0.05$) and paired T test ($p<0.05$) showed significant difference among the samples and, between the seasons respectively, indicating variation of water chemical composition. PCA results revealed that chemical composition in C1 was dominated by SO_4^{2-}, U and K in rainy season while pH, Cl^-, and U dominated C1 in dry season, C2 and C3 were dominated by HCO_3^- and SO_4^{2-} in rainy season while, in dry season, C2 was dominated by Ca^{2+}, Mg^{2+}, Na^+, Fe, Si, HCO_3^- and SO_4^{2-}, and C3 negatively correlated with major ions. Further, water type results indicate C1 (mixed cation-HCO_3^-), C2 (Ca- HCO_3^--SO_4^{2-}) and C3 (Ca-Mg- HCO_3^-) characteristics in rainy season while, in dry season, shows C1 (mixed cation- HCO_3^--Cl^-), C2 (Ca-HCO_3^-) and C3 (Ca-Mg- HCO_3^-). Normalized Na^+/ HCO_3^- and Mg^{2+} /Ca^{2+} molar ratios suggest dominance of silicate weathering and mixing of silicate and carbonate weathering products controlling river water chemistry. Inverse models and SI results revealed main reactions as dissolution of calcite, plagioclase, biotite, feldspars with carbon dioxide and pyrite consumption; kaolinite, iron (III) hydroxides and quartz. High NO_3^-/Na^+ and SO_4^{2-}/Cl^- molar ratios were recognized in C2 and C3 samples in both seasons respectively, showing impact of anthropogenic activities from agricultural and industrial sources. Uranium levels in river water attributed to presence of uranium minerals, however, uranium speciate into $Ca_2UO_2(CO_3)_3$ and $UO_2(CO_3)_2^{2-}$. Consequently, all samples were within WHO guidelines for major chemical constituents except pH and Fe in some samples.

Keywords: Hierarchical Cluster Analysis, Principal Component Analysis, Kayelekera

TABLE OF CONTENTS

LIST OF FIGURES

LIST OF TABLES

LIST OF ABBREVIATIONS

AAS	Atomic Absorption Spectrometry
APHA	American Public Health Association
BG	Borosilicate Glass
BGS	British Geological Survey
EC	Electrical Conductivity.
EIA	Environmental Impact Assessment
EPA	Environmental Protection Agency
HCA	Hierarchical Cluster Analysis
ICP - AES	Inductively Coupled Plasma – Atomic Emission
ISO	International Standard Organization
MBS	Malawi Bureau of Standards
PC	Principal Component
PCA	Principal Component Analysis
TSF	Tailing Storage Facilities
WHO	World Health Organization

CHAPTER 1

INTRODUCTION

1.1. Background

The availability of quality water is an essential prerequisite for sustainable development (Aksonye *et al*., 2007) because of its many uses that support ecosystems and human life (Sherif *et al.,* 2018). Rivers constitute the main inland water resource for domestic, industrial and irrigation uses in many areas (Varol *et al.,* 2011). However, rivers are vulnerable water bodies because of their role in carrying off and assimilating pollutants from both point sources (e.g., municipal wastewater and industrial discharge) and non-point sources (e.g., agricultural, and urban runoff, atmospheric deposition) (Carpenter *et al.,* 1998; Ouyang *et al.,* 2006). In addition, rivers are affected by seasonal variation which alters concentration of different pollutants through surface rainfall and runoff (Vega, 1998). As a result, information on river water quality and pollution sources is important for the implementation of sustainable water-use management strategies (Barakat *et al*, 2016; Crosa *et al.,* 2006; Sarkar *et al*., 2007; Zhou *et al*., 2007).

Natural processes and anthropogenic activities such as agricultural and other land uses (Caccia & Boyer, 2005; Zhang *et al.,* 2007), and sewage discharge (Arain *et al.,* 2008; Gantidis *et al.,* 2007; Kundewicz *et al.,* 2007), water-rock interaction (Prasanna *et al*., 2011) degrade the quality of fresh surface waters, and hence, impair their use for domestic,

industrial, agricultural, and recreational purposes (Arain *et al*., 2008; Carpenter *et al*., 1998; Gantidis *et al*., 2007; Jarvie *et al.*, 1998; Kundewicz *et al*., 2007). In this regard, it imperative to have reliable information on spatial and temporal variations of water quality (Varol et *al.*, 2011) to forestall water pollution (Razmkhah *et al*., 2010; Subramani *et al*., 2010; Senthilkumar *et al.*, 2012).

Malawi is endowed with a variety of freshwater systems (Makwinja et al., 2019), including Lake Malawi, Lake Malombe, Lake Chilwa, Shire River, and several networks of river systems such as Lilongwe River, Dwangwa, Bua, Linthipe, Ruo, South and North Rukulu, and other small streams (Kumambala, 2010). Numerous studies have been conducted on river water quality across Malawi (Phiri et al. (2005), Dryton (2008), and Nyasulu (2008). However, only few studies focused on rivers found in the Northern part of Malawi.

1.2. Problem statement

The Kayelekera area is a mountainous watershed area that makes a significant contribution of water recharged into North Rukuru River, one of the major inputs to Lake Malawi, in Northern Malawi. The area also hosts a suspended uranium mining operation. Due to its rural setting, the communities depend on rivers as main source of water supply for domestic and agricultural use. In this regard, the quality of water resources has a bearing on both the communities and ecosystems, including Lake Malawi. However, there is paucity of studies that report on the state of water quality and the hydro-geochemical processes that control that quality in the area. The lack of the knowledge is a major concern of uncertainty in understanding the quality of the available water and the processes controlling the water chemistry and poses a problem in management of water. Therefore, this study will close the knowledge-gap of surface water quality around the Kayelekera area in relation to hydro-geochemical processes and water use problems in the area. In addition, the study will identify the source(s) of contamination around the area. In so doing, the study will help in development of appropriate management strategies essential to minimize potential public health risks (Carroll *et al*., 2008).

1.3. Research Objectives

1.3.1. General objective

The aim of the study was to examine the state of water quality in rivers and streams in the head waters of the North Rukuru River, one of the major tributaries to Lake Malawi, in Northern Malawi.

1.3.2. Specific Objectives

Specifically, the objectives of the study were:

1. To investigate the status of water quality physiochemical parameters of the rivers across the rainy and dry seasons.
2. Identify key sources of contaminants in the rivers of the study area
3. To evaluate geochemical processes associated with degradation of water quality of rivers in the study area.

1.4. Justification of the study

The results of the study will serve as baseline information on surface water quality in terms of some selected physio-chemical parameters and involved hydro geochemical processes in the study area. The study will assist in advising government on policy regarding surface water use in the country and advise on monitoring of surface water quality for both domestic and commercial use in the country. Further, the results will help the Government of Malawi to achieve the objective to promote sustainable water resources development and management with a view to facilitating an equitable provision of adequate quantity and quality of water for all users. A study of seasonal and temporal variability assessment of surface water quality in Kayelekera will reveal the concentrations of different surface water quality parameters which will provide a basis for optimized water resources management,

quality monitoring activities and enhanced treatment rates. Identifying sources of solutes and hydro geochemical processes involved will help water management planners to find efficient methods for water treatment in area. As such, the study is very important in maintaining public health and the wellbeing of households.

1.5. Organization of the thesis

Chapter one contains the introduction of the thesis that includes background, problem statement, and research objectives. Chapter two provides literature related to water quality and hydro geochemical processes. Chapter three describes the study area, and methods used in the study. Chapter four presents the findings of the study area. It discusses results of hydrochemistry, seasonal and spatial variation, principal component analysis, hierarchical cluster analysis, surface water types and geochemical modelling. Chapter five summaries main issues and provides recommendation for further research.

CHAPTER 2

LITERATURE REVIEW

2.1 Water quality assessment in rivers

Water quality is defined by the physical, chemical, and biological characteristics and composition of water (Hounslow, 1995; Panchani *et al*., 2013; USGS, 2005), related to different uses of water such as drinking, irrigation or recreation or environmental requirements (Cordoba *et al.,* 2010). The physical and chemical parameters that define river water quality include dissolved oxygen, temperature, pH, electrical conductivity (EC), nitrates, phosphates, and sulphates (Wetzel & Likens, 1991). The presence of different chemical and physical parameters more than their permissible limits for various uses create health hazards and environmental problems (Al-Zahah *et al.,* 2007). Hence, analysing water quality parameters is critical in assessing water consumed by the population against the required water quality standards (Amfo-out *et al.,* 2014).

Electric conductivity (EC) in water is a measure of the capability of water to pass electrical flow (Environmental Protection Agency, 2001). Dissolved solutes such as calcium, magnesium, sodium, potassium, bicarbonate, nitrate, sulphate, and chloride occur in the form of electrically charged ions (Nyarko, 2008; Shinde *et al.,* 2011). As such, EC is an indirect measure of ionic strength and mineralization of natural water (Murungesan *et al*., 2006; Nyarko, 2008; Papazotos *et al.,* 2019), and indicates the level of inorganic dissolved

solids (Healey, 2014). While pH affects geochemical processes such as adsorption/desorption, solubility of minerals and speciation of trace metals in water (Kwame, 2011), and therefore toxicity to aquatic life (Mansouri, 2011).

The composition of major ions in natural waters (e.g., K^+, Na^+, Ca^{2+}, Mg^{2+}, Cl^-, SO_4^{2-}, and $HCO_3^-$is used to understand processes leading to loading of chemical solutes into surface water bodies, and local processes that affect water chemistry, such as rock weathering, evaporation/crystallization, and atmospheric precipitation (Xu *et al.*, 2010; Zhang *et al*., 2012). However, with poor management of pollution sources like untreated sewerage and agricultural runoff, may lead to pollution of surface water bodies. For example, elevated values of Cl^- are highly related with landfill sites, urban centers, and irrigation agricultural (Srinivasamoorthy *et al*., 2008).

2.2 . Sources of riverine solutes

The major sources of riverine solutes may be categorised as natural processes (e.g., rock mineral weathering, atmospheric deposition, groundwater inflows) and anthropogenic inputs (e.g., agricultural, and industrial activities, urbanization) (Gibbs, 1970; Meybeck, 2003). The water chemistry may then be modified along the course through the chemical, biological and physical processes such as redox reactions, cation exchange, evaporation concentration, and precipitation of secondary minerals (Jones *et al*., 1998; Mohan *et al*., 2000; Mulligan *et al.*, 1997; Postma 2005 *et al*; Reddy *et al*., 2010; Reddy and Kumar 2010; Raju *et al*., 2011; Satyanarayanan *et al.*, 2007; Tirumalesh *et al*., 2010).

2.2.1. Weathering and erosion

Weathering and erosion processes such as chemical weathering of soils/rocks and mechanical erosion supply dissolved and particulate loads to rivers. Generally, chemical weathering of rocks in a drainage basin is largely controlled by carbonate and silicate weathering (Edmunds & Smedley, 2000; Karim & Veizer, 2000; Quade *et al*., 2003; Singh *et al*., 2005). Weathering reactions require acidity (H^+ ions). Carbonic acid is accepted as the major weathering agent, however, whereas the importance of other acids (sulphuric, nitric, or organic acids) as an agent is gradually recognized (Karim & Veizer, 2000; Li *et*

al., 2008b; Spence & Telmer, 2005;). In reducing organic-rich environments such as wetlands, wastewater ponds, and landfill leachates, acidity may be derived from bacteria mediated degradation of organic matter and oxidation of sulphide [H_2S] and ammonia [NH_4^+] in soils, producing sulphuric acid and nitric acid, respectively (Table *1*). Other sources of sulphuric acid include the oxidation of atmospheric SO_2 emitted from anthropogenic activities such as coal combustion (Larssen *et al.*, 2006) and bacteria mediated oxidation of sulphide minerals such as pyrite (Fe_2S). Pyrite is commonly present in coal shales, sandstones, and igneous rocks, and can be a component of tailings from mining operations.

The sources of CO_2 in soils are atmospheric CO_2 and the decomposition of organic matter during periods of high biological activity and root respiration (Rasse *et al*., 2001). Carbon dioxide then combines with water to form carbonic acid, which is a source of protons. Therefore, the amount of carbonic acid in water depends on the pCO_2 in the atmosphere and soils and increases in soils due to respiration (Appelo & Postma, 2005). In unsaturated soils, weathering proceeds under open system conditions, because CO_2 and O_2 diffuse continuously into the water from soil air or atmosphere. Studies done by Jiang *et al.*, (2015) analysed the variation of hydrochemistry in the upper Yangcun Hydrologic Station of the Yarlung Tsangpo and concluded that the CO_2 consumption caused by chemical weathering of silicate and carbonate in this area showed a significant contribution to the corresponding global values. In contrast, closed system conditions exist in the saturated zone, where CO_2 and O_2 are limited to the levels dissolved in recharge, and the resultant water chemistry is characterised by high pH. However, weathering proceeds faster under open system conditions, resulting in higher concentrations of solutes.

Table 1: Reactions of formation of acid for mineral dissolution (from Appelo and Postma, 2005)

Source	Reaction(s)
Carbonic acid from atmospheric CO_2	$CO_2 + H_2O \rightarrow \ H^+ + HCO_3^-$
Carbonic acid from respiration	$CH_2O + O_2 \rightarrow HCO_3^- + H^+$
	$(CH_2O)_n + nO_2 \rightarrow nH_2O + nCO_2$
	$CO_2 + H_2O \rightarrow H_2CO_3$
Atmospheric SO_2 oxidation	$SO_2 + 2OH^- \rightarrow H_2SO_4 \rightarrow SO_4^{2-} + 2H^+$
Sulphuric acid from sulphide oxidation	$H_2S + 2O_2 \rightarrow SO_4^{2-} + 2H^+$
Nitric acid from nitrification	$NH_4^+ + 2O_2 \rightarrow NO_3^- + H_2O + 2H^+$
Sulphuric acid from pyrite oxidation	$FeS_2 + 3¾O_2 + 3½H_2O \rightarrow Fe(OH)_3 + 2SO_4^{2-} + 2H^+$
Ferrous iron oxidation and hydration	$Fe^{2+} + ¼O_2 + 2½H_2O \rightarrow Fe(OH)_3 + 2H^+$

The contribution of the acidity reactions to water chemistry is reflected in the concentrations of the corresponding anions, which are limited by thermodynamics (solubility limitation) and kinetics of weathering of solid phases (Harrison, 1999). For instance, bicarbonates, silica, calcium, and sodium may be derived from the weathering of plagioclase, while magnesium and potassium may be derived from the relatively less weatherable feldspars (Hudson & Golding, 1997). On the other hand, new solid phases may form by precipitation of low solubility minerals such as calcite (Appelo & Postma, 2005; Harrison, 1999; Stumm & Morgan, 1996;).

2.2.1.1. Silicate weathering

Silicate minerals, which form most of the Earth's crust, comprise a series of silicate and aluminium-silicate minerals such as quartz [SiO_2], ferromagnesian silicates (e.g., olivine [$(Fe, Mg)_2SiO_4$], pyroxene [$Ca(Mg, Fe)Si_2O_6$], biotite [$(Mg, Fe)_3(AlSiO_{10})(OH)_2$], amphibole {$Ca_2(Na)(Mg, Fe, Al)_5[(Al, Si)_4O_{11}]_2(OH)_2$}, and feldspars (e.g., anorthite [$CaAl_2Si_2O_8$], albite [$NaAlSi_3O_8$], labradorite [$(Ca, Na)(Al, Si)_4O_8$], orthoclase [$KAlSi_3O_8$], and muscovite [$KAl_2(AlSi_3O_{10})(OH)_2$]). The weathering of these silicate minerals is estimated to contribute approximately 45 % of the total dissolved load of the world's rivers (Stumm and Wieland 1990; Stumm and Wollast, 1990). Besides the global riverine fluxes of solutes, weathering also contributes to the long-term CO_2 cycle (Gaillardet *et al.*, 1999).

The rate of weathering of silicate minerals is slow and varies with the silicate mineral as depicted by the Goldich sequence (Colman, 1982; Goldich, 1938), which reflects the overall chemical kinetic control on the distribution of primary silicate minerals during weathering (Table 1). Olivine and Ca-plagioclase are listed as the most easily weatherable minerals, and quartz as the mineral most resistant to weathering (Aiuppa *et al.*, 2000; Appelo and Postma, 2005).

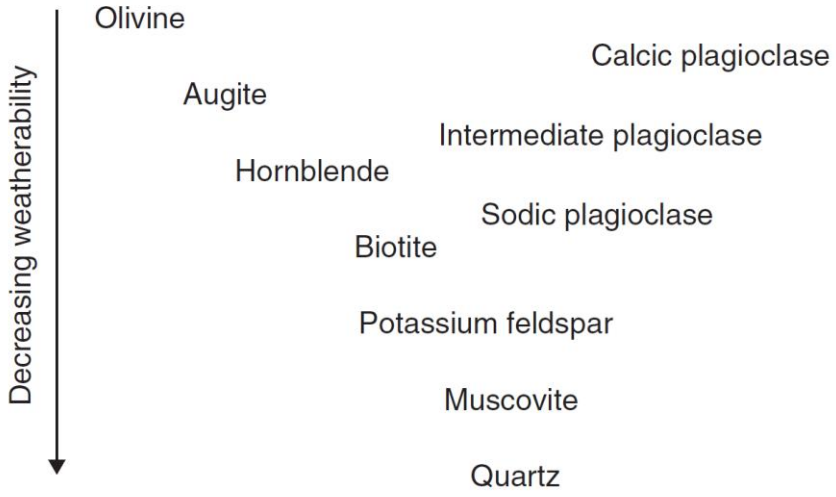

Figure 1:The Goldich weathering sequence based on observations of the sequence of their disappearance in soils (Goldich, 1938). Adapted from Appelo and Postma (2005).

Weathering reactions for some common primary minerals are listed in Figure 1, where the clay mineral kaolinite is used as an example of a weathering product (Appelo & Postma, 2005; Bricker *et al*., 1968; Das & Kaur, 2001; Garrels & Mackenzie, 1967; Négrel & Lachassagne, 2000; Sarin *et al*., 1989; Singh and Hasnain 1999). Kinetics of the weathering mineral, in combination with hydrological conditions, determines the nature of the weathering product. For example, montmorillonite is a favoured product in the weathering of rapid weathering volcanic rocks in relatively dry climates (i.e., where there is low rate of leaching of the soil). Gibbsite, on the other hand, typically forms in tropical areas with intense rainfall and well drained conditions, removing silica and cations from the primary silicates (Appelo & Postma, 2005).

Table 2:Weathering reactions for different silicate minerals to the clay mineral kaolinite (from Appelo and Postma, 2005)

Sodic plagioclase (Albite)	*Kaolinite*
$2Na\,(AlSi_3)\,O_8 + 2H^+ + 9H2O$	$\rightarrow\ Al_2Si_2O_5(OH)_4 + 2Na^+ + 4H_4SiO_4$
Calcic plagioclase (Anorthite)	
$Ca\,(Al_2Si_2)\,O_8 + 2H^+ + H_2O$	$\rightarrow\ Al_2Si_2O_5(OH)_4 + Ca^{2+}$
K-feldspar (Microline)	
$2K(AlSi_3)\,O_8 + 2H^+ + 9H_2O$	$\rightarrow\ Al_2Si_2O_5(OH)_4 + 2K^+ + 4H_4SiO_4$
Pyroxene (Augite)	
$(Mg_{0.7}CaAl_{0.3})\,(Al_{0.3}Si_{1.7})\,O_6 + 3.4H^+ + 1.1H_2O$	$\rightarrow\ 0.3Al_2Si_2O_5(OH)_4 + Ca^{2+} + 0.7Mg^{2+} + 1.1H_4SiO_4$
Mica (Biotite)	
$2K(Mg_2Fe)\,(AlSi_3)\,O_{10}(OH)_2 + 10H^+ + 0.5O_2 + 7H_2O$	$\rightarrow\ Al_2Si_2O_5(OH)_4 + 2K^+ + 4Mg^{2+} + 2Fe\,(OH)_3 + 4H_4SiO_4$

Olivine	
$(Mg, Fe)_2SiO_4 + 4H^+$	$\rightarrow 2\ Mg^{2+} + 2Fe^{2+} + H_4SiO_4$
Carbonic acid	
$CO_2 + H_2O$	$\rightarrow\ H^+ + HCO_3^-$
Sulphuric acid	
H_2SO_4	$\rightarrow\ 2H^+ + SO_4^{2-}$
Nitric acid	
HNO_3	$\rightarrow\ H^+ + NO_3^-$

The aluminium silicates undergo incongruent weathering, forming clay minerals (montmorillonite and kaolinite) and gibbsite, due to the insolubility of Al-compounds, and releases cations (Ca^{2+}, Na+ and K^+) and silicic acid (H_4SiO_4) to solution (Brantley *et al*., 2014; Fletcher *et al*., 2006). On the other hand, weathering of Al-free ferromagnesian silicates, such as pyroxene and olivine, proceeds congruently releasing Mg^{2+}, Fe^{2+} and silicic acid to solution (Freeze & Cherry, 1979; Deutsch, 1997). As these minerals contain no aluminium, clay minerals like kaolinite do not form (**Error! Reference source not found.**). As can be seen from Table 2, silicate weathering primarily affects water chemistry by increasing cations, silica, and pH. Under natural conditions, carbonic acid and organic acids are the most important sources of protons, leading to production of bicarbonate (Table 1). However, under polluted conditions, sulphuric acid and nitric acid may play a role (Li *et al*., 2008; Zhang *et al*., 2020).

$$2Na_xK_{(1-x)}AlSi_3O_8 + H_2SO_4 \rightarrow 2Na^+ + 2(1-x)\ K^+ + SO_4^{2-} + 6SiO_2 + 2AlOOH \quad (1)$$

$$2Na_xK_{(1-x)}AlSi_3O_8 + H_2CO_3 \rightarrow 2Na^+ + 2(1-x)\ K^+ + 2HCO_3^- + 6SiO_2 + 2AlOOH \quad (2)$$

Further, if iron is present, from either silicate minerals that contain iron (e.g., biotite and/or hornblende) or pyrite oxidation, iron may form insoluble Fe-oxides (Appelo and Postma, 2005). For the alkali feldspars, the concentrations of Na^+ and K^+ can be used as an

indication of the extent of weathering, as there are few mineralogical controls on their concentrations. For anorthite, Ca^{2+} concentrations are generally limited by calcite saturation. In natural waters, values of silica are more commonly in the range of 10 to 30 ppm, despite its high solubility, because of low rate of silicate mineral weathering and sorption of silicic acid on mineral surfaces and organics in soils.

2.2.1.2. Carbonate weathering

Carbonate minerals are ubiquitous, not just as limestone and dolomite formations, but also as cements filling fractures in silicate rocks, and crusts in soils. Weathering of carbonate rocks proceeds more rapidly than weathering of silicate rocks. Therefore, much of the watershed geochemistry of most of the world's major rivers is dominated by the weathering of carbonates (Chen *et al*., 2002; Gaillardet *et al*., 1999; Hu *et al*., 1982; Langmuir, 1997). In general, the principal reactions for dissolution of calcite and dolomite are:

$$CaCO_3 + H^+ \rightarrow Ca^{2+} + HCO_3^- \quad (3)$$

$$CaMg(CO_3)_2 + 2H^+ \rightarrow Ca^{2+} + Mg^{2+} + 2HCO_3^- \quad (4)$$

Specifically, in the case where the acidity is derived from carbonic acid, then

$$CaCO_3 + CO_2 + H_2O \rightleftharpoons Ca^{2+} + 2HCO_3^- \quad (5)$$

$$Ca_x Mg_{(1-x)} CO_3 + H_2O + CO_2 \rightleftharpoons x\,Ca^{2+} + (1-x)\,Mg^{2+} + 2HCO_3^- \quad (6)$$

In this case, the amount of carbonate dissolved is ultimately controlled by partial pressure of CO_2 of the system and limited by the saturation of calcite (Amiotte-Suchet *et al*., 1995; Hiscock, 2004; Lerman *et al*., 2007; Probst *et al*., 2000; Vries *et al*., 2003; Xu and Liu, 2010). Whereas, in the case where the acidity is derived from sulphuric acid and nitric acid, then the reactions are (Xu and Liu, 2007):

$$2Ca_xMg_{(1-x)}CO_3 + H_2SO_4 \rightarrow 2xCa^{2+} + 2(1-x)\,Mg^{2+} + 2HCO_3^- + SO_4^{2-} \quad (7)$$

2.2.2. Mining activities and waste disposal

Mining operations generate large volumes of solid waste and wastewater, which may be present onsite as overburden and tailing ponds, respectively. Tailings contain minerals

from the host rock and by-products of the beneficiation process (Burri 2019; Ntengwe & Maseka, 2006). During high rainfall events, highly contaminated tailings may form part of runoff, and wastewater ponds may spill over, polluting nearby rivers (Ashton, 2001). Further, chemicals such sulphuric acid used in the beneficiation process may spill, leak, or leach from the mine site into nearby water bodies.

Mine operations exploiting base metal sulphide and relatively sulphide-rich coal deposits will generate sulphide-bearing tailings, such as pyrite (FeS_2), which are unstable when exposed to atmospheric oxygen and undergo oxidation (Nordstrom & Alpers 1999; Smith & Huyck, 1999; Stumm & Morgan 1981):

$$4FeS_2 + 15O_2 + 14H_2O \rightarrow 4Fe(OH)_3 + 8SO_4^{2-} + 16H^+ \quad (8)$$

The net reaction renders the water in the system more acidic (Kleinmann *et al.,* 1981; Nordstrom 1982; Singer & Stumm, 1970; Williamson & Rimstidt, 1995) and it's implicated in generation of acid mine drainage (AMD). The lowering of pH increases solubility of range of minerals, releasing toxic chemicals into water bodies (Jambor & Blowes, 1998; Udayabhanu & Prasad, 2010). However, when sulphide minerals other than pyrite are subject to weathering, they do not necessarily produce acidity, but cations and SO_4^{2-} ions are still released into the environment (Younger *et al.,* 2002). For example, studies of surface water quality in the Tibetan rivers have reported elevated levels of heavy metals such as Hg, Cd, Ni, Cu because of contamination from local mining industry (Huang *et al.,* 2009; Li *et al.,* 2007).

Domestic sewage and leachate from solid waste dumpsites may contain ammonia because of their highly reducing conditions. Mixing of such wastewater with oxygen-rich river water would cause oxidation of ammonium ions to nitrates, in the presence of ammonium and nitrite oxidizing microorganisms according to following reactions (Galloway, 2003):

$$2NH_4^+ + 2O_2 \rightarrow 2NO_2^- + 2H_2O + 4H^+ \quad (9)$$

$$2NO_2^- + O_2 \rightarrow 2NO_3^- \quad (10)$$

Therefore, the concentration of dissolved nitrate in the river water would increase. Generally, the HNO_3 and H_2SO_4 acids dissolve minerals and accelerate chemical

weathering of rocks (Barnes and Raymond, 2009), which introduces more solutes into water, that causes environment and health problems.

2.2.3. Land use and land cover

Human activities such as agricultural development, biomass burning and human settlements result in changes in land cover (Calder *et al*., 1995). Changes in the land cover and land management practices are key influencing factors behind the alteration of the hydrological system, such as the timing, amount and sediment load of runoff generated in a catchment (Bai & Ouyang, 2010; Ellery et al., 2010; Kaspersen et al., 2016; Tang, *et al*., 2011; Teutschbein *et al*., 2018). In addition, runoff from agricultural land carries pesticides, herbicides, and nutrients such as such as nitrogen and phosphorus from fertiliser application to rivers (Walmsley, 2000; Worrall & Burt, 1999; Zobrist & Reichert, 2006).

Many studies have shown that there are significant correlations between land use and water quality indicators (Baker, 2003; Buck *et al*., 2004; Chu *et al*., 2013; Li *et al.*, 2008; Schoonover *et al.*, 2005; Sliva & Williams, 2001; Tong & Chen 2002; Woli *et al*., 2004). Most of these studies conclude that agricultural land use strongly influences stream water nitrogen (Arheimer & Liden, 2000; Johnson *et al.*, 1997; Smart *et al*., 1998), phosphorus (Arheimer & Liden, 2000; Hill, 1981), and suspended solids (Allan *et al.*, 1997; Johnson *et al*., 1997). For example, the expansion of farmland and city areas has a positive effect on the increase in the concentration of total phosphate (Wang *et al*., 2014) and grassland and forest areas are negatively correlated with the concentrations of NO_3^- and SO_4^{2-} ions in water (Zhao *et al.*, 2015). In addition, under the pressure of increasing population, economic development, and changes in land use patterns, the original hydrogeochemical characteristics of many rivers have undergone alterations (Chen *et al*., 2005; Ometo *et al*., 2010; Zhang *et al.*, 2015b), especially rivers that are influenced by urban areas (Connor *et al*., 2014; Kaushal *et al*., 2017; Merchán *et al.*, 2015; Rose, 2007). Noteworthy examples of such rivers are the Seine, Rhine, Weser, and Elbe Rivers in Europe, the Mississippi and St. Lawrence Rivers in North America, and the Minjiang and Huai Rivers in China (Gaillardet *et al*., 1999; Qin *et al.*, 2006; Zhang *et al*., 2011).

2.3. Uranium geochemistry in surface water

In natural waters, uranium minerals usually exist in two main oxidation states: the soluble hexavalent U(VI) or the insoluble tetravalent U(IV)) form (Langmuir, 1978). The fate and the transport of uranium are governed by the contrasting chemistry of U (IV) and U (VI). Abiotic factors such as ions and minerals strongly influence the migration process of uranium (Barnett et al., 2000; Arnold et al., 2001; Duff et al., 2002; Baik et al., 2004). For example, U (VI) generally forms soluble, and thus mobile, complexes with carbonate and hydroxide, while U (IV) precipitates as the highly insoluble mineral uraninite (Nyman et al., 2006). Oxidized uranium, U (VI), is highly soluble and toxic, and thus is a potential contaminant to local drinking-water reservoirs (NABIR, 2003).

The environmental geochemistry of uranium has been studied in detail and has been summarized in several review articles (e.g., Abdelouas 2006; Wall & Krumholz 2006). The studies found that U(IV) species form under reducing conditions has also a higher affinity for surface binding sites and a lower solubility than U (VI) species (Langmuir, 1978). The product of U (VI) reduction is often uraninite (UO_2) (Campbell et al., 2011; Finch and Murakami, 1999; Langmuir, 1997). In oxygenated aqueous systems, uraninite rapidly oxidizes to the U (VI) species as the uranyl ion, UO_2^{2+}, (Rabinowitch & Belford, 1964) which is highly soluble and stable over a wide pH range (Murphy and Shock, 1999). Uranyl ions UO_2^{2+} forms carbonate complexes of varying stoichiometry as a function of the pH and the partial pressure of CO_2(g) i.e., UO_2CO_3, $UO_2CO_3{}_2^{2-}$, or $UO_2(CO_3)_3^{4-}$ (Brookins, 1988). Uranyl carbonates are highly soluble and play a dominate role in the migration of uranium in neutral to alkaline water (Finch and Murakami, 1999).

Simultaneously, sorption and precipitation of uranyl largely impact its mobility (Ilton et al., 2008) and electron transfer reactions leading to its sequestration (Jeon et al., 2004; Liu et al.2006; Kelly et al., 2008). Studies have shown that uranium (VI) sorbs to a variety of minerals and related phases including clays (Rodriguez et al., 2008; Whicker et al., 2007), iron (oxy) hydroxides (Duquene et al., 2008; Gómez et al., 2006; Martinez et al., 1995; Sherman et al., 2008) and aluminium and silica oxides (Sylwester et al., 2000). Iron minerals have extensively shown to be efficient sorbents of U (VI), both in the laboratory and in subsurface sediments (Catalano & Brown, 2005). Sorption of U (VI) by iron

hydroxides retards its mobility during the oxidative weathering of ore deposits (Murakami et al., 1997; von Gunten et al., 1999; Allard et al., 1999). In other studies, the adsorption of U (VI) to clay minerals was observed to be more complex, due to the larger variety of potential sorption sites (McKinley et al., 1995; Turner et al., 1996). The adsorption of U (VI) to other pure mineral phases such as sulfides (Wersin et al., 1994) and carbonates (Morse et al., 1984) have also been investigated; studies showed that the complexes were less stable and less soluble.

However, U (VI) adsorption is very sensitive to pH, and carbonate and calcium concentrations (Curtis et al., 2006; Davis et al., 2004; Fox et al., 2006). Aqueous complexation of U (VI) with carbonate ions decreases the tendency of U (VI) to bind to mineral surfaces (Elzinga et al., 2004; Guillaumont et al., 2003; Hsi & Langmuir, 1985; Waite et al., 1994), thus enhancing the mobility of uranium (Duff & Amrhein, 1996; Wang et al., 2004). The formation of calcium–uranyl–carbonate complexes further reduce adsorption potential (Bernhard et al., 2001; Dong & Brooks, 2006; Fox et al., 2006, Hyun et al., 2009; Kelly et al., 2007; Nair & Merkel, 2011; Stewart et al., 2010). Sorption decreases in the presence of complexing ligands such as humic and fulvic acids, and in the presence of competing cations such as Ca^{2+} and Mg^{2+} (Park, 2005).

2.4. Analysis of hydro-geochemical data for evaluation of river water chemistry

2.4.1. Hydro-geochemical modelling

Hydro-geochemical modelling involves a conceptual model coded into a computer program to understand the processes involved in evolution of natural water chemistry (Belkhiri *et al*., 2010; Federico *et al*., 2008; Lecomte *et al*., 2005; Sharif *et al*., 2008), such as dissolution and precipitation of mineral phases (Appelo & Postma, 1993; Engesgaard & Kipp, 1992; Eraifej , 2006; Gandhi *et al*., 2002; Keating & Bahr, 1998; Kohler *et al.*, 1996; Lichtner *et al*., 2004; Molinero *et al.*, 2004; Parkhurst, 1995; Plummer *et al.*, 1988; Robinson *et al*., 2000; Saaltink *et al*., 2003; Samper & Ayora, 1994; Sun *et al*., 2001; Xu *et al*., 1999; Yeh & Triparthi, 1989; Yeh, 2000; Zhu & Anderson, 2002). The computer programs are based on equilibrium chemistry of aqueous solutions interacting with minerals, gases, solid solutions, exchangers and sorption surfaces and kinetically

controlled reactions and transport along flow path (Felmy *et al*., 1984; Helgeson *et al.*, 1970; Parkhurst *et al*., 1990; Plummer *et al*., 1976; Shannon *et al*., 1977; Spostigo & Mattigod, 1979, Truesdell & Jones, 1973; Wolery, 1979). Examples of the computer programs for aqueous geochemical calculations include MINTEQA2 (Allison *et al.*, 1990; WATEQ4F (Nordstrom, 2007), JESS (May and Murray, 2008), PHREEQC (Parkhurst and Appelo, 2005) and PHAST (Parkhurst, 2010).

PHREEQC is a computer program written in C programming language to perform a variety of low temperature aqueous geochemical calculations. It is based on an ion-association aqueous model and has capabilities for speciation and saturation-index calculations, batch-reaction and one-dimensional transport calculations involving reversible and irreversible reactions, which include aqueous, mineral, gas, solid solution, surface-complexation, and ion-exchange equilibria, and specified mole transfers of reactants, kinetically controlled reactions, mixing of solutions, and pressure and temperature changes; and inverse modelling, which finds sets of mineral and gas mole transfers that account for differences in composition between waters within specified compositional uncertainty limits (Parkhurst & Appelo, 2005).

Inverse modelling may also be implemented in computer codes, such as NETPATH, for modelling net geochemical reactions along a flow path (Plummer *et al*., 1994). However, these inverse geochemical models were limited in that mass transfers were constrained by the stoichiometry of the reactions which lead to statistical bias and underestimation of uncertainty (Dai *et al*., 2004; Neuman, 2003; Ye *et al*., 2004). Parkhurst (1995, 1997) presented a statistically based approach that accounts for inaccuracies in the analysis and uncertainties in the set of reactions. This approach was implemented in PHREEQC v.2 (Parkhurst & Appelo, 1999). PHREEQC (Parkhurst & Appelo, 1999) and is based on a geochemical mole-balance model which calculates the phase mole transfers (the moles of minerals and gases that must enter or leave a solution) as a result of the observed difference between initial and final water compositions along the flow path. The mass balance conceptual model is represented as follows (Li, *et al.*, 2010)

$$\sum_{j=0}^{n} aijxj = bj \qquad (11)$$

Here, a_{ij} is the atomic figure of element *i* in mineral *j*, x_j is the molar figure of minerals or gases that dissolve or precipitate (degas) in solution, and b_j expresses the augment of element *i* from one site to another site. If the values are greater than 1, it indicates that minerals or gas dissolve; otherwise, precipitation or outgassing occurs. Recent references with applications of PHREEQC inverse modelling to geochemical problems, include Uliana and Sharp (2001), who used inverse modelling to study groundwater evolution along the flow path and spring discharge under base flow and stormflow conditions; and Eary *et al*., (2003), who assessed water quality changes in connection with mining operations. Drever (1997) includes a chapter on the use of popular computer codes to assess water quality problems through transport and reaction modeling. Perry (2001) described the reactions between water and rock by inverse modelling in a waterlogged coal mine in Appalachia, USA. Therefore, inverse modelling accounts for the chemical changes that occur as water evolves along a flow path.

The implication of computer programme in calculation of equilibrium distribution of inorganic species of major and minor elements in natural waters using chemical analysis and in situ measurements of EC, pH were discussed in detail by Truesdell and Jones (1973). Helgeson et al. (1970), Plummer et al. (1976), Shannon et al. (1977), Spostigo and Mattigod (1979), Wolery (1979), Felmy et al. (1984), Parkhurst et al. (1990) and many others have developed a variety of geochemical models for describing and deducing the chemical behaviour of complex and mixed waters. Several earlier workers have also used geochemical models for solubility equation study of water (Wolery 1979; Wolery 1983; Tamata 1990; Deutsch 1997; Elangovan 1997; Murphy & Schramke, 1998). A brief review of existing geochemical studies has been given by Nordstrom et al. (1979), Jenne (1981), Plummer et al. (1983), Runnels (1978) and Plummer et al. (1990).

2.5. Statistical methods

Statistical methods such as principal component analysis (PCA) and cluster analysis (CA) have the capability of analysing large amounts of data and distinguishing complex relationships among many variables (Jalali, 2010). Therefore, these statistical methods are required to interpret large and complex dataset generated by assessment of multiple water quality parameters (Li *et al.*, 2011) to identify possible sources, natural and/or

anthropogenic factors, that influence the quality of water resources (Gatica *et al*., 2012; Liu *et al.*, 2011). As a result, statistical methods are tools for management of water resources as well as effective solutions to pollution (Kazi *et al.*, 2009; Kumar *et al*., 2009; Razmkhah *et al*., 2010; Varol & Sen, 2009).

Several studies have investigated hydro geochemistry of river systems in different areas around the globe by using multivariate analysis. For example, Edet *et al*., (2013) conducted a study on hydro geochemistry of the river systems in the southeastern Nigeria using multivariate statistics. The results showed that tidal flushing and dumping of domestic and human waste into the river systems were the main factors controlling the river water chemistry with little or no contribution from silicate and carbonate weathering. Song *et al*., (2011) applied multivariate statistical analysis to evaluate water quality of a tributary of the Pearl River, southern China. They concluded that most variables in the agricultural/rural area were primarily influenced by physicochemical and organic pollution, sewage pollution, geogenic factor, agricultural non-point source pollution, and accumulated pesticide usage while in the industrial/ urban area were related to industrial wastewaters, mineral contamination, geogenic factor, urban sewage, and chemical industrial pollution. Jung *et al*., (2016) evaluated the water quality for the Nakdong River watershed using multivariate analysis.

2.5.1 Principal Component Analysis (PCA)

PCA provides information on the meaningful parameters, which describe the whole data set through data reduction with a minimum loss of original information (Helena *et al.*, 2000; Singh *et al*., 2004; Vega *et al*., 1998). PCA explains the variance of the data set with inter-correlated variables and, transform the variables into a smaller set of independent uncorrelated variables called principal components (PC). The PCs are obtained by multiplying the original correlated variables with the eigenvector, which is a list of coefficients (loadings or weightings) (Jollife, 2016; Varol *et al*., 2012).

The principal components are extracted such that the maximum variance is dedicated to the first component, the second greatest variance to the second component, and so on (Purushothaman *et al.*, 2014). Usually, the minor PCs can be eliminated to simplify the

analysis because of their poor interpretation of the data structure (Yeung, 1999). The principal component (PC) is expressed as:

$$z_{ij} = a_{i1}x_{1j} + a_{i2}x_{2j} + a_{i3}x_{3j} + \ldots + a_{im}x_{jm} \qquad (12)$$

Where z is the component score, a is the component loading, x the measured value of variable, i is the component number, j the sample number and m the total number of variables. PCA use absolute values of factor loadings along with a ruleset based on the spread of variance among principal component (PC) axes to determine relative information content in each variable (Nauman *et al.,* 2009). To test the suitability of the data for PCA, Kaisere Meyere Olkin (KMO) and Bartlett's Sphericity tests are performed on the parameter correlation matrix. KMO is a measure of sampling adequacy that indicates the proportion of variance that might be caused by underlying factors. A high value (close to 1) generally indicates that PCA may be useful. Bartlett's test of sphericity indicates whether the correlation matrix is the identity matrix, which indicates that the parameters are unrelated (Shrestha and Kazama, 2007).

2.5.2 Cluster Analysis

Cluster analysis categorizes entities (e.g., sampling sites) into distinct groups or clusters maximising within-group similarity maximized, and among-group dissimilarity (Templ *et al.*, 2008). As a result, cluster analysis reveals the intrinsic pattern of similar objects within a data set without making a prior assumption about the data (Kassambara, 2017; Vega *et al.*, 1998). The traditional clustering methods may be categorised into two approaches called partitioning and agglomerative clustering. Partitioning clustering approaches subdivide the data sets into a set of *k* groups, where *k* is the number of groups pre-specified by the analyst. The commonly used partitioning clustering include *K*-means clustering (MacQueen, 1967), in which, each cluster is represented by the means of the data points belonging to the cluster, *K*-medoids clustering (Kaufman & Rousseuw, 1990), in which, each cluster is represented by one of the objects in the cluster, and Clustering Large Applications (CLARA) algorithm, which is an extension to *K*-medoids adapted for large data sets. The *K*- medoids clustering method is less sensitive to anomalous data points and outliers.

Hierarchical cluster analysis (HCA) is an alternative approach to partitioning clustering for grouping objects based on their similarity (McKenna, 2003). In contrast to partitioning clustering, hierarchical clustering does not require the number of clusters to be specified prior to the analysis. Hierarchical clustering can be subdivided into agglomerative clustering and divisive clustering. In agglomerative clustering, each observation is initially considered as a cluster of its own (leaf). Then, the most similar clusters are successively merged until there is just one single big cluster (root). On the other hand, divisive clustering is an inverse of agglomerative clustering. It begins with the root, and then the most heterogeneous clusters are successively divided until all observation is in their own cluster.

The classification of observations into groups requires computing the distance or the (dis)similarity between each pair of observations. The classical methods for distance measures are Euclidean and Manhattan distances. The choice of distance measures is a critical step in clustering, as it has a strong influence on the clustering results. For most common clustering software, the default distance measure is the Euclidean distance. Other dissimilarity measures exist such as correlation-based distances, such as Pearson, Spearman, Eisen cosine (Eisen *et al.*, 1998) and Kendall correlation distances. Pearson correlation, the most used method, is a parametric correlation which measures the degree of a linear relationship between two profiles. Kendall and Spearman correlations are non-parametric, and they are used to perform rank-based correlation analysis. It's generally recommended to standardize the variables before distance matrix computation to make variables, which are measured in different scales, comparable.

In HCA, the level of (dis)similarity between objects is visualized using a dendrogram, a multilevel hierarchy where clusters at one level are joined together to form the clusters at the next levels (Davis, 1986, Shrestha *et al*., 2007). The dendrogram provides a visual summary of clustering process, presenting a picture of groups and their proximity, making it possible to decide the level at which to cut the tree for generating suitable groups of a data objects (Bodrud-Doza *et al*., 2016; Machiwal & Jha, 2015). In understanding water chemistry, several other studies have successfully implemented HCA using Euclidean distance as the (dis)similarity measure, together with Ward's method as the linkage rule to produce a dendrogram with the most distinctive groups (Cloutier *et al.*, 2008; Güler *et al.*,

2002; Lambrakis *et al*., 2004; Monjerezi *et al.,* 2011; Templ *et al*., 2008; Wanda *et al*., 2011). Ward's method uses an analysis of variance approach to evaluate the distances between clusters to minimize the sum of squares of two clusters are formed at each step. Commonly, Statistical software is used to implement the HCA and PCA such as R statistical software (R Development Core Team, 2009), Minitab (Minitab. Inc, 2010) and SIMCA-P+ (Umetrics, 2013).

Various studies used CA and PCA for instance, Phung *et al.,* (2015) used CA and PCA to evaluate temporal/spatial variations of surface water quality in Can Tho City, a Mekong Delta area of Vietnam. Kumarasamy *et al*., (2014) used CA and PCA to investigate the hydrochemistry of a Tamiraparani river basin, Southern India. Khan *et al.,* (2016) applied CA to hydrochemical data to assess spatial variability in the water quality of Ramganga River and its tributaries (Ganga Basin, India). Correlation analysis and PCA and CA components were used by Sharma *et al*., (2015) to study the seasonal variation, identify potential sources of pollution, and clustering of monitoring stations of Ganga and Yamuna Rivers in Uttarakhand State (India). Other works were conducted using PCA and CA (Bouza-Deano *et al*., 2008, Kazi *et al.,* 2009, Hai *et al*., 2009, Razmkhah *et al*., 2010b; Simeonov *et al.,* 2003). Furthermore, other studies (Boyacioglu & Boyacioglu, 2007; Liu and Guo, 2007; Zhang *et al.,* 2009; Zhou,) applied the PCA and CA methods to classify the sampling sites and to identify the latent pollution source. All above studies showed that the PCA and CA statistical methods are important tools to determine underlying relationships between the water quality parameters, identify sources of pollution, and group similar monitoring stations into clusters with similar characteristics.

CHAPTER 3

MATERIALS AND METHODS

3.1. Description of study area

3.1.1. Topography, drainage, and climate

The Kayelekera area is in Karonga district, Malawi (Figure 2), in undulating hills of lower elevations of the Great East African Rift escarpment, a dominant topographic unit of the area (Ray, 1975). The Karonga Rift scarp zone rises abruptly from the lakeshore plain unit through a fault scarp. The dissected hills of the zone have elevations between 610 and 1180 m above sea level. Locally, elevations rise from about 760 m in the Sere River valley to about 2120 m at the summit of Mususi Hill to the southwest of Kayelekera (Bowden, 2007).

The principal drainages of the study area are North Rukuru River, Sere River, Chapwasha River, Kantchindu River, Chimembe River, Champhanji River and Muswanga River (Figure 3). The Sere and Muswanga Rivers are perennial and are both tributaries to the North Rukuru, a main perennial river in the study area (Atkins, 1990). The Sere River has a catchment of approximately 156.5 km². It is formed by confluence of Luwembe and Mapambo Rivers, which originate in basement material to the north-west of the study area, then it is joined by the Chapwasha River (originating in the Musisi Forest reserve) and the Nakatangala River (flowing from the north) and then flows in a south-easterly direction through Karroo sediments then into the North Rukuru, which is seated on basement

materials. The Champhanji, Chimembe and Kantchindu Rivers are also tributaries to the Sere River. However, the upper reaches of the Champhanji, as well as the entire Chimembe and Kantchindu Rivers are ephemeral, whereas the lower reaches of the Champhanji are perennial (Atkins, 1990). The Muswanga River originates in the basement outcrops, high in Musisi Forest reserve, to the south-west and flows into the Karroo sediments in the study area. It has a catchment approximately a third of the size of the Sere River catchment, at 46, 8 km² (Atkins, 1990).

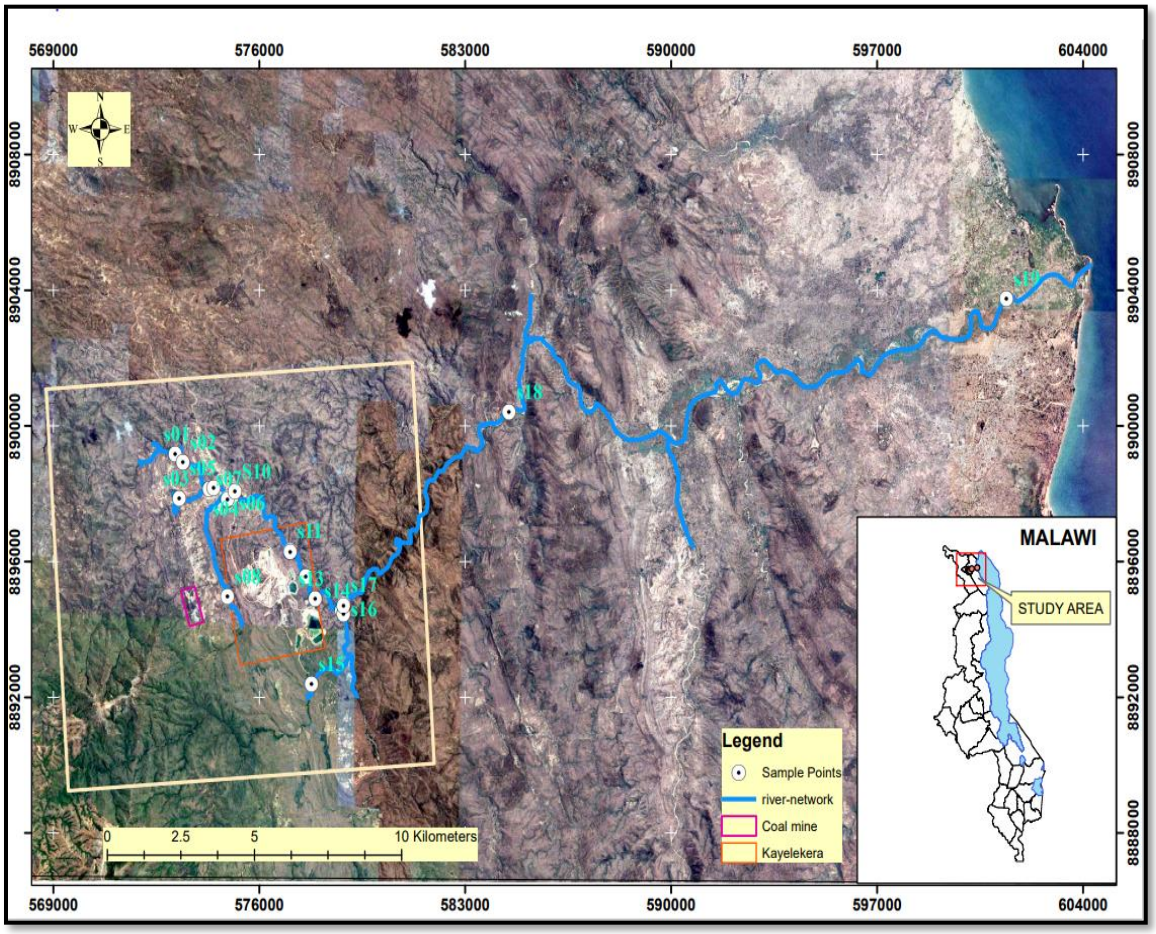

Figure 2: Study area

The study area has a tropical wet and dry "savanna" climate (MetMalawi, 2006), characterised by a distinct rainy season between November and April. The local climate of the Kayelekera site is influenced by its locality on the rift valley escarpment, 200 to 500 m higher than Lake Malawi. The mean annual evaporation (1685 mm) exceeds mean annual

precipitation (960 mm) for the site, with average monthly temperatures ranging between 20 and 30 ^{o}C.

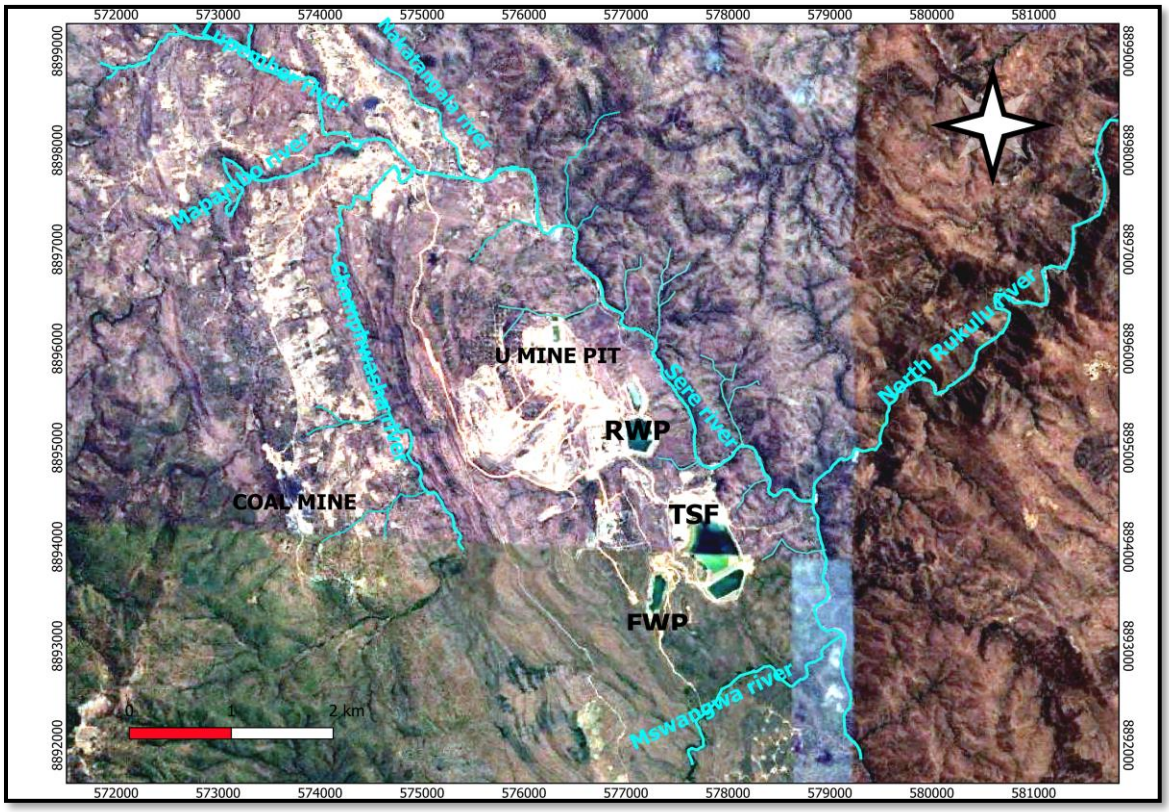

Figure 3: Map showing land cover of the study area

3.1.2. Land use

Main land uses are agricultural production and mining of coal and uranium. The most valuable farming lands are in small valleys and troughs between the hills, and the gentle slopes (Figure 3). The area is covered with grassland savannah flanked with riverine woodland on a sloping ridge between streams on the southern and northern sides (Figure 3).

The Kayelekera area also hosts a uranium mine along the Sere River and coal mine along Chaphwasha River (Figure 3). The uranium mine is the largest mining operation in the area and was designed to process 1.5 million tonnes per annum of raw material by grinding, acid leaching, resin-in-pulp extraction, elution, precipitation and drying to produce a final product (uranium concentrate) called "yellow cake". It operated from May 2008 until February 2014 when production was suspended, with the operation placed on care and maintenance. The site comprises an open pit, a uranium extraction plant and storage facilities of different types of waste produced by the mine, such as waste rocks placed into waste rock dumps and marginal ore dumps, and the mill such as tailings placed into Tailings Storage Facilities (TSF). The tailings are stored in "TSF A" located in the south-east of the mine site on the right bank of the Sere River catchment (Figure 3) in Kantchindu valley (EIA report, 2006).

3.1.3. Geology and Soil

The Karonga area is mainly underlain by metamorphic and igneous rocks of the pre-Karroo Malawi basement complex (Figure 4). These are overlain by several small basins of Karroo sediments and, nearer to Lake Malawi, by Cretaceous to recent lacustrine sediments (BGS, 2009). The major lithological components of the basement complex are micaceous and amphibole-bearing gneisses (Carter & Bennet, 1973; Shluter, 1997). The Karroo sediments are found in several grabens and mainly comprise arkosic sandstones and carbonaceous, pyritic shales with thin coal seams near to the base overlain by calcareous mudstones and limestones (Ray, 1975; Atkins, 1990). The arkoses contain microcline, perthite, plagioclase, quartz, chert, polycrystalline quartz, biotite, muscovite, mudstone pellets, and carbonaceous material associated with pyrite (Bowden & Shaw, 2007; Wilde *et al*., 2019).

In the mudstones, smectite is the dominant clay constituent together with minor kaolinite and white mica, with the kaolinite more dominant at or near the surface. The lower arkoses are characterised by a primary oxide (hematitic) matrix partially altered to geothite/limonite on weathering or primary reduced (chlorite/pyrite) and abundant carbonaceous debris (Wilde *et al.,* 2019).

Kayelekera is one of several significant uranium deposits within Karoo-aged sandstones of eastern Africa, but it is the only one that achieved production (Bowden and Shaw, 2007). Approximately 50% of the total uranium ore occurs in primary reduced (i.e., carbon and pyrite-bearing) arkose, 30% of the ore is hosted in oxidized arkose (i.e., lacking carbon and pyrite). The remaining ore is hosted in mixed arkose, exhibiting characteristics of both primary and secondary arkose ore types, and in mudstones (Bowden & Shaw, 2007). Uranium in primary ore is present as coffinite, minor uraninite, disseminated in matrix clay, included in detrital mica grains and intimately intergrown with carbonaceous matter. The oxidized arkose units are found at or near the current surface and in peripheral parts of the deposit (Hellman & Schofield, 2006) and are characterized by feldspar deterioration, prevalence of iron oxide, and a matrix of smectite and illite. The reduced ore is most prevalent in the lower arkose units and contain fresh feldspars and carbonaceous debris with pyrite and chlorite. Calcite is a significant component of the primary reduced ore (Wilde et al., 2019). The mudstone mineralogy is dominated by smectite and illite. Secondary uranium is often most concentrated at contacts with adjacent mudstones. Coal is the other economically recoverable resource other than uranium within the Kayelekera mineralisation. (Atkins, 1990; Carter *et al.*, 1973; Ray, 1975). The coal is present in the study area in deposits at the Kayelekera uranium deposit and Nkhachira, located approximately 3 km to the west (Atkins, 1990).

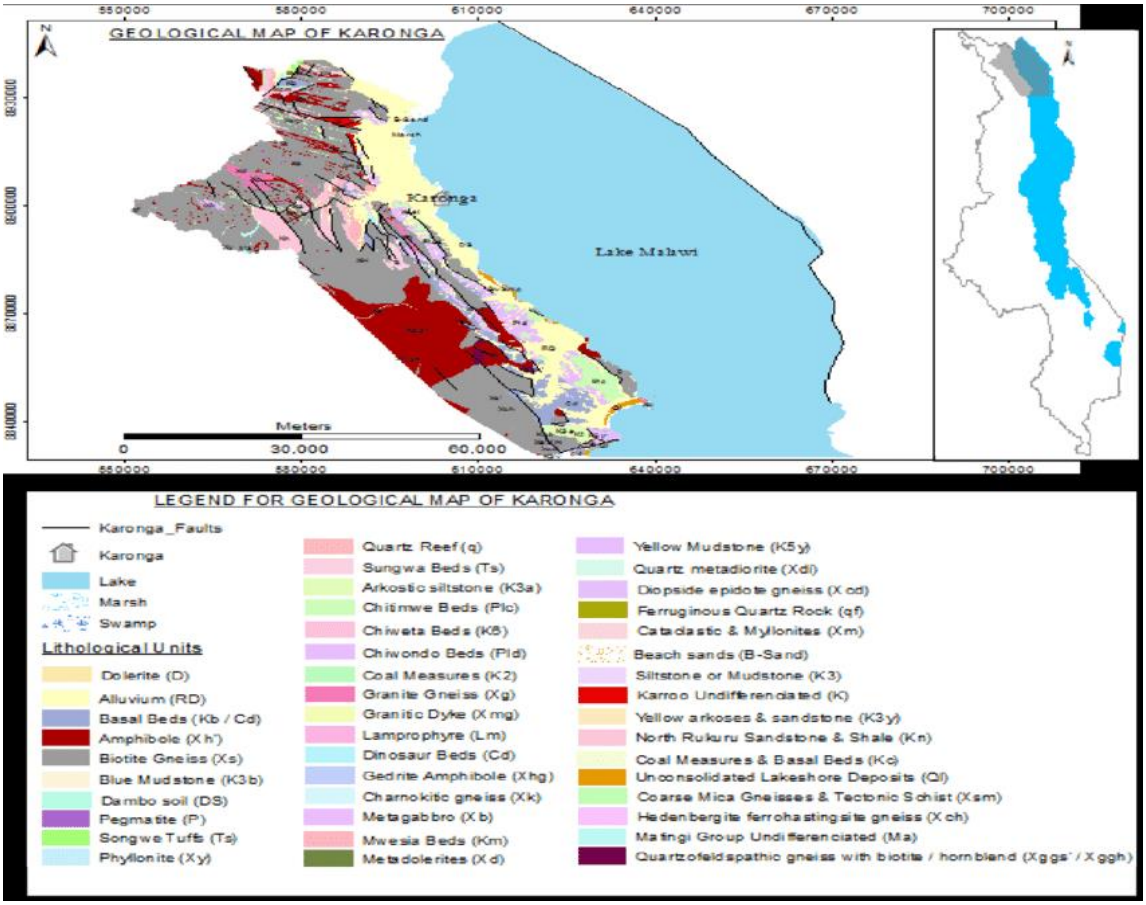

Figure 4: Geological features of the study area (insert is Map of Malawi showing location of Karonga).

The soils of the Kayelekera area may be categorised into basement and Karoo soils based on the parent material. The basement soils are relatively shallow, and they are present in the lower Kantchindu, Chimembe, and Sere River valleys (Atkins, 1990). The Karoo soils show significant differentiation based on textural and drainage characteristics (Atkins, 1990), and are further classified as arkose unit, mudstone unit and dambo soils. Dambo soils are saturated for much of the time and some soils have high organic matter content (Ray, 1975). The exchange complex of most soils is dominated by calcium, with high magnesium and potassium content, especially in mudstone unit soils which is ascribed to weathering of montmorillonite clays containing magnesium and potassium (Atkins, 1990).

3.2. Sample collection and preparation

Field surveys were carried out within the study area to identify sampling sites and their attributes. Water samples were collected from a selection of sites on the main rivers in the Kayelekera area (Figure 2) using standard sampling procedures (ISO 5667:1993; USEPA, 1999). At each sampling site, pre-cleaned new polyethylene bottles (500 ml) sample bottles were rinsed three times with water from the respective sampling point before collecting the actual sample. GPS coordinates were collected at each sampling site using a Garmin GPS 60 CSx.

A duplicate set of samples were collected at each site. One set of water samples was then acidified with HNO_3 (to pH <2) and sample bottles tightly capped placed in double plastic bags and stored at 4^oC until metal analysis to prevent biodegradation of metals. Samples for anion analysis were collected in triplicates (in 500 ml), and strictly kept at 4^oC in a portable fridge until further processing in the lab. The acidified sample was filtered through 0.45µm membrane filters and transferred into two unused 125 mL pre-cleaned HDPE bottles for cation-and trace element

analysis using ICP-OES. The unacidified sample was unfiltered and transferred into 125 mL unused pre-cleaned HDPE bottles for analysis of major anions and total alkalinity.

3.3. Water sample analysis

3.3.1 Determination of pH, DO, EC and TDS

All samples were measured for physical characteristics and analysed for main chemical components using standard methods (APHA, 2005). Values of pH, total dissolved solids (TDS), oxidation reduction potential (ORP), dissolved oxygen (DO) and temperature were measured in the field. pH was measured (ISO 10523-1:1994) using a pH meter (826 pH mobile metrohm model), dissolved oxygen was measured using DO meter (HI 98293, Hanna) while TDS (ISO 7888:1985) and temperature of the surface water samples were determined using a temperature/EC/TDS meter (Mettler Toledo).

3.3.2 Determination of Chlorides and Carbonates

Titrimetric methods were used to determine the concentration of chlorides ($AgNO_3$) and carbonates (acid) (EPA, 1994). The concentration of sulphates was determined turbidimetrically (barium sulphate; APHA, 2005). NO_3–N was determined (2, 6-dimethylphenol method) followed by spectrophotometric method (EPA, 2011).

3.3.3 Determination of trace metals

Major cations (Na^+, Ca^{2+}, Mg^{2+}, K^+) and U concentrations were determined using inductively coupled plasma atomic emission spectroscopy (ICP-OES) while atomic absorption spectroscopy (AAS) was used for Fe analysis. The instrument was calibrated using five calibration solutions ranging 0-5 mg/L for Fe, Mn, K and 0-25 mg/L for Na, Mg, and Ca. The standards prepared for the ICP-OES analysis were applied for calibration curve.

3.3.4 Data Analysis

All statistical analyses were performed using R: A language and environment for statistical computing version 4.1.2 (R Core Team, 2021). The paired *t*-test and one-way ANOVA were performed on all measured parameters across the seasons and sample points to show spatial-temporal variation of river water quality (Elbag, 2006; Pallant, 2013). The chemical variation (Fataei, 2011) in all water samples was analysed using Hierarchical Cluster Analysis (HCA) and Principal Component Analysis (PCA). For the HCA, the water quality data were standardised using the R base *scale* () function and then Euclidean distances were calculated using R base *dist* () function as a measure of dissimilarity. The *hclust* (stats package) function was used to create the hierarchical tree using "Ward.D2" linkage method (Ward, 1963) and the dendrograms for data from rainy and dry seasons were visualised and compared using *tanglegram* (dendextend package; Galili, 2015) function.

PCA was performed using *PCA* function in FactoMineR package (Lê *et al*., 2008) to link correlations among water quality parameters to the sample points (Gajbhiye *et al*., 2011). The PCA and all other biplots between chemical parameters were produced using ggplot2

package (Wickham, 2016) for visual evaluation. A correlation matrix for physicochemical water quality properties was produced using *rcorr* (Hmisc package, Harrell, 2021), incorporating Spearman's correlation. The correlation matrix was displayed using *corrplot* (corrplot package, Wei & Simko, 2021) and ordered by hierarchical clustering (Friendly, 2002; Murdoch & Chow, 1996), using "Ward.D2" method (Ward, 1963).

The geochemical modelling program PHREEQC v3 (Parkhurst & Appelo, 2013), implemented with MINTEQ.v4 database (Allison *et al*., 1991) was used to calculate saturation indices with respect to mineral phases. The same program was utilised to calculate speciation of uranium by considering the most abundant inorganic ligands in water (OH^-, Cl^-, SO_4^{2-} , HCO_3^- and CO_3^{2-}) to check the mechanisms of uranium mobilisation. Inverse and forward geochemical models were also formulated in PHREEQC v3 to account for observed changes between the identified principal groups of water samples along the river course.

CHAPTER 4

RESULTS AND DISCUSSION

4.1. River water quality and spatiotemporal variation of solutes

Distribution of major physical and chemical parameters is presented in Figure 5, whereas all data are presented in Appendix 1. pH ranged from 7.28 to 8.61 and 7.79 to 8.83, with 10% and 20% of the samples exceeding drinking water guideline (pH = 8.5; WHO, 2008) in the rainy and dry seasons, respectively. All samples show low mineralisation, with values of TDS ranging between 33.80 to 260.79 mg/L (mean = 115.66 mg/L) and 33.80 to 260.79 (mean = 117.69 mg/L) in rainy season and dry season, respectively (Figure 5). Levels of dissolved oxygen (DO) were within the required range (> 5 mg/L) (WHO, 2008; USEPA, 2001) in both rainy (5.96 to 8.06 mg/L) and dry (6.42 to 8.06 mg/L) seasons.

All samples did not exceed WHO guidelines for sulphates (500 mg/L), nitrates (50 mg/L), chlorides (250 mg/L), calcium (150 mg/L), magnesium (50 mg/L) and potassium (60 mg/L), sodium (200 mg/L) and uranium (0.03 mg/L). Concentrations of bicarbonate (HCO_3^-) ions ranged from 25 to 105 mg/L and 23 to 100 mg/L in rainy and dry season, respectively (Figure 5). Levels of Fe exceeded WHO water quality guidelines (0.02 mg/L) in six samples collected in the rainy season (Figure 5). Levels of Fe were generally higher ($p < 0.05$) in the rainy season than dry season, whereas levels of Cl^- and Na^+ were higher ($p < 0.05$) in the dry season (Figure 5).

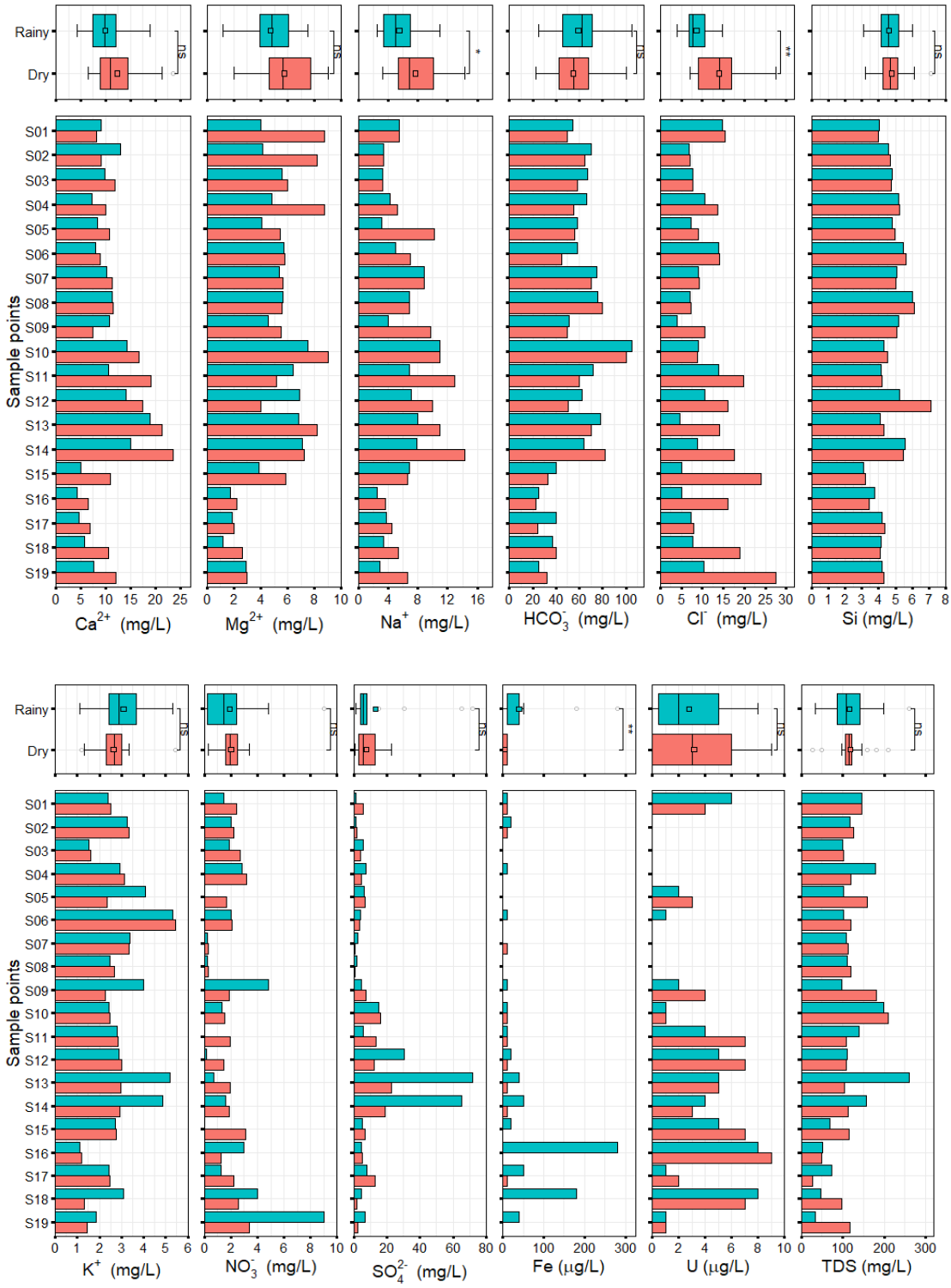

Figure 5: Distribution of analysed physicochemical parameters in the river water sampled in the rainy and dry seasons.

Spatially, pH, Si, Mg^{2+}, Ca^{2+}, Na^{+}, K^{+}, SO_4^{2-}, HCO_3^{-}, TDS, Fe and U varied significantly across the sampling points. Therefore, hierarchical clustering analysis (HCA) was able to group the samples into three clusters in each season, based on their chemical characteristics. In general, cluster 1 (C1) comprises downstream samples, C2 midstream and C3 comprises upstream samples with a good season overlap (Figure 6). The samples in the first cluster have lowest mineralization (Figure 5; average TDS = 717 mg/L) and are characterised by a mixed cation-HCO_3^{-} composition in the rainy season, which changes to mixed cation- HCO_3^{-}-Cl^{-} composition in the dry season associated with a slight increase in TDS (Figure 6). In the rainy season, these samples also show relatively higher levels of iron and nitrates (Figure 5). These are mainly distributed in North Rukuru River (Figure 2). C2 comprises a small number of sample (Figure 2) located mid-section of the Sere River, in the vicinity of TSFA (Figure 3). These samples have relatively high mineralisation (Figure 5; average TDS = 106mg/L) and sulphate content in the rainy season (Figure 5). They are characterised by a Ca-HCO_3^{-} composition in the dry season and a Ca-HCO_3^{-}-SO_4^{2-} composition in the rainy season. Samples in C3 have intermediate mineralisation with a Ca-Mg- HCO_3^{-} composition in both seasons (Figure 5). These samples are mainly found in the upper reaches of the study area, in Luwembe River, Chaphwasha River, Mapambo River, and top part of Sere River (Figure 2). Samples in C1 and C2 also show relatively elevated levels of uranium in both seasons (Figure 5).

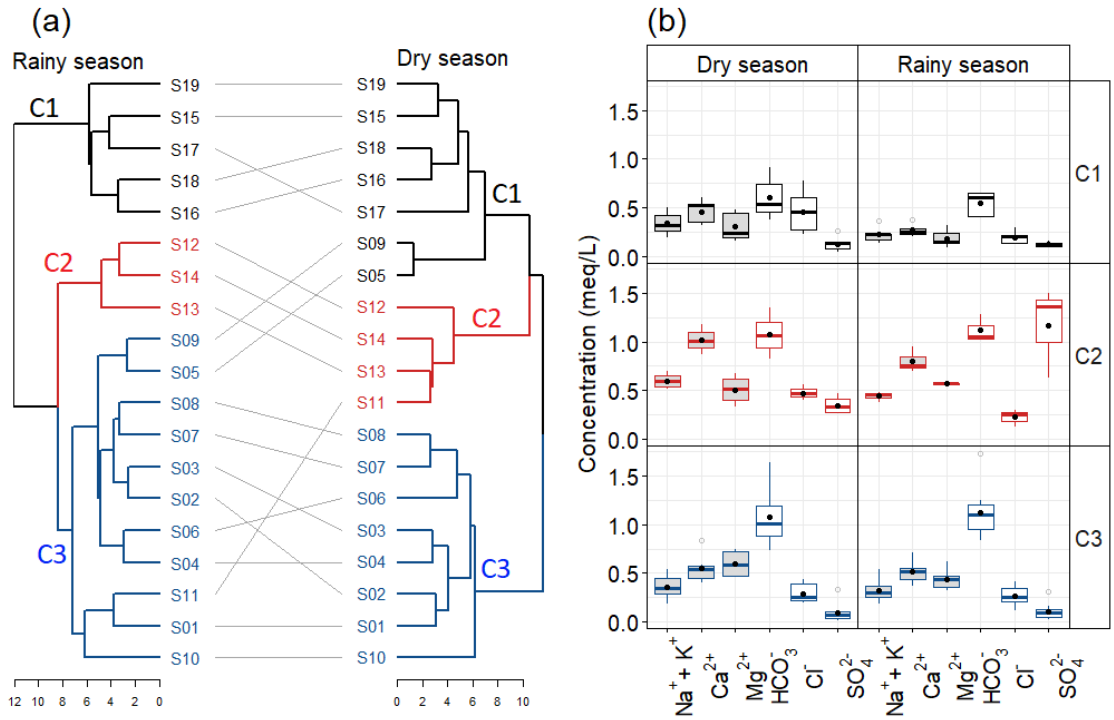

Figure 6:(a) Dendrogram showing clustering of sampling locations based on surface water characteristics in the Sere River and its Catchment for the rainy and dry seasons. (b) Boxplots of surface water of three clusters in both rainy and dry season.

In the rainy season, HCO_3^-, SO_4^{2-}, the major cations and silica are the major determinants of TDS. Using hierarchical clustering, the chemical parameters can be grouped into two main hierarchical clusters: HCO_3^-, SO_4^{2-}, the major cations and silica (alongside TDS); and uranium alongside iron (Figure 6). The major cations (Na^+, Ca^{2+}, Mg^{2+}) were positively correlated to each other and to HCO_3^-, silica and TDS. Uranium concentrations were positively correlated with iron levels. In contrast, a negative correlation was found between the aqueous concentrations of bicarbonate with iron and uranium, nitrates with sodium, and silica with uranium (Figure 7). PCA gave five principal components (PCs), with eigenvalues ≥1 (Kaiser, 1958), which accounted for 84% of the total variance. The first two components (PC1 and PC2) accounted for >50% of the variation and are shown in Figure 8. In PC1, which explains 37.8% of the variance, the major cations, HCO_3^-, SO_4^{2-}, and silica (alongside TDS) are the dominant variables with the highest positive value, whereas iron and nitrates had the highest negative values. Positive sample scores along PC1 are typically high for water samples in C2 and C3, whereas samples in C1 a negative

score (Figure 8). PC2, which explained 16.02% of variance, constituted positive correlations with pH, sulphate, potassium, and uranium, but was negatively correlated with chlorides. PC2 is mainly associated with positive scores for C2 samples and their neighbouring C1 samples (high sulphate, uranium and potassium, (Figure 8), and negative scores for C3 samples (Figure 8).

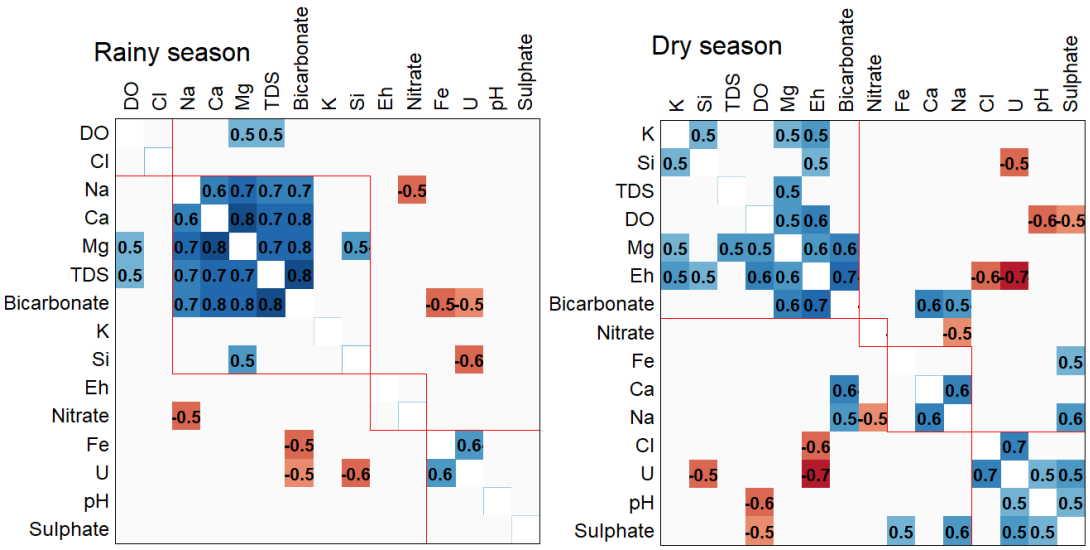

Figure 7: Correlation matrices of chemical water quality parameters for the samples collected in rainy and dry seasons. Only significant Spearman's ρ values ($p < 0.05$) are shown. Variables are ordered by hierarchical clustering and red squares enclose clusters, s showing closely related physicochemical parameters.

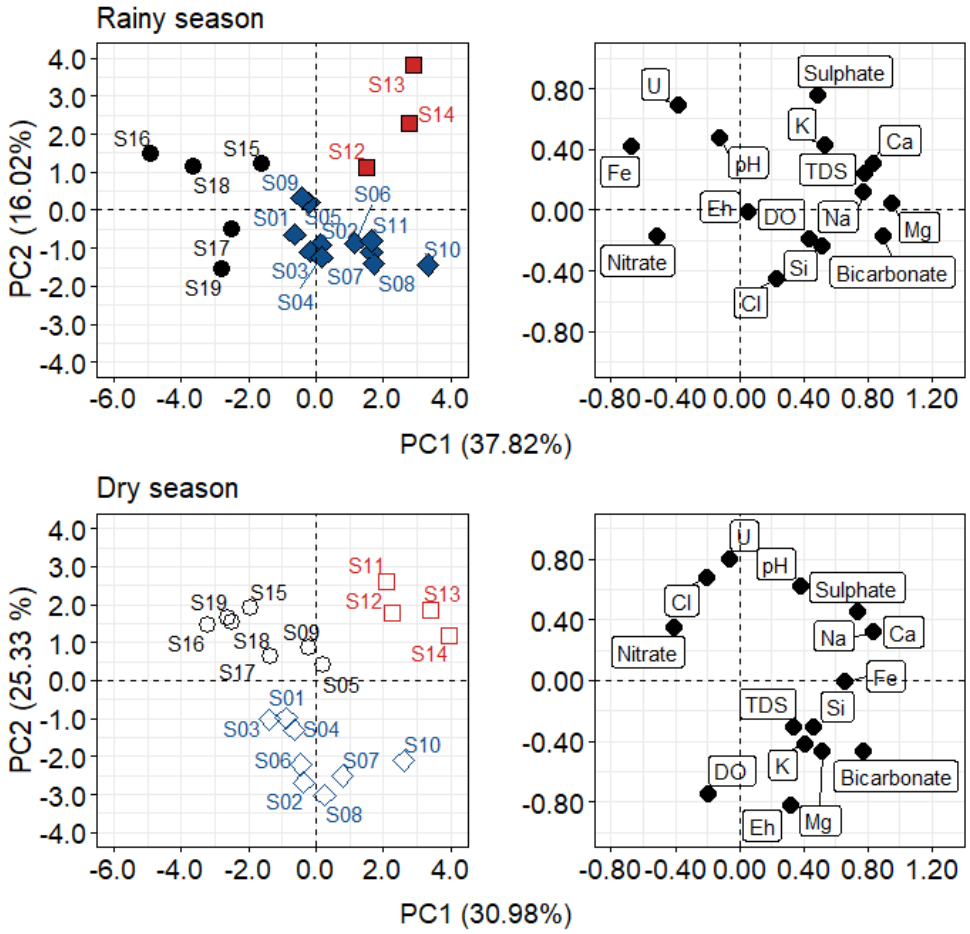

Figure 8: Results of PCA showing the first two PCs explaining >50% of variance in water chemistry. Samples are grouped according to their HCA clusters (See. Figure 6).

In the dry season, the PCA and correlation analysis show the major cations (Na^+, Ca^{2+}, Mg^{2+}) positively correlated to HCO_3^-. In addition, Mg^{2+} is correlated to K^+ and TDS, Ca^{2+} and Na^+ to each other, and Si with K^+ (Figure 7). Uranium concentrations were positively correlated with levels of Cl^-, pH and SO_4^{2-}, but negatively correlated with Si and redox potential. Further, SO_4^{2-} levels were positively correlated with Fe, Na^+ and pH, whereas Na^+ had a negative correlation with nitrates (Figure 7). PCA gave four principal components (PCs), with eigenvalues ≥1 (Kaiser, 1958), which accounted for 76.49% of the total variance. The first two components (PC1 and PC2) accounted for >50% of the variation and are also shown in Figure 8. In PC1 (30.98% of variance), Ca^{2+}, Mg^{2+}, Na^+, Fe, Si, HCO_3^- and $SO_4^{2-}$are all positively correlated with this dimension. Positive sample

scores along PC1 are typically high for water samples in C2, whereas samples in C1 have negative scores along this dimension (Figure 8). PC2 (25.3%) constituted positive correlations with pH, chloride, and uranium, but was negatively correlated with DO, Mg^{2+} and HCO_3^-. PC2 is mainly associated with positive scores for C2 samples and their neighbouring C1 samples and negative scores for C3 samples (Figure 8).

4.2. Major sources and controls of solutes in river water

In general, dissolved solutes that constitute river water chemistry may come from natural processes, such as atmospheric input, mineral weathering, mixing with groundwater, and anthropogenic activities including agricultural, and industrial activities (Gaillardet *et al*., 1999; Gibbs, 1970; Meybeck, 2003).

4.2.1. Chemical weathering

A first indication of possible sources of solutes may be gained from consideration of levels and ratios of main chemical components (weatherable minerals and dissolved major cations) and description of land use of the study area (Fairchild *et al*., 1994; Tranter *et al*., 2002; Wadham *et al.,* 2010). For weathering processes, Na^+-normalized molar ratios of HCO_3^- and Mg^{2+} to Ca^{2+} may be used to show the relative importance of carbonate, silicate and evaporite dissolution (Gaillardet *et al*., 1999). In this study, the river waters cluster around the silicate endmember, while a scatter (of mainly C3) towards carbonate endmember is also observed (Figure 9), suggesting domination of silicate weathering and the mixing of silicate and carbonate weathering products in controlling the river water chemistry.

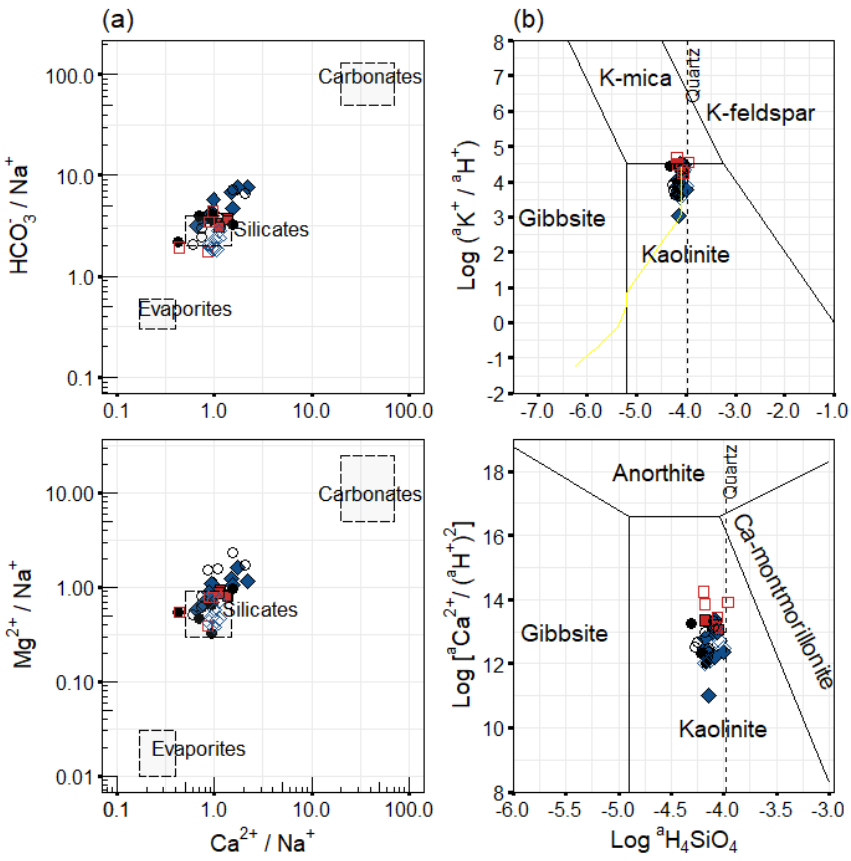

Figure 9 : (a) Mixing diagrams using Na^+-normalized ratios of Ca^{2+} (Ca^{2+}/Na^+) and Mg^{2+} (Mg^{2+}/Na^+) in river water. (b) Logarithmic activity diagrams depicting equilibrium phase relationships among stoichiometric minerals and aqueous solution in the CaO-Al_2O_3-SiO_2-H_2O and K_2O-Al_2O_3-SiO_2-H_2O system at 25 ^{o}C, 1 bar, unit activity of H_2O. Stability data for solid phases are from thermodynamic data given in Postma and Appelo (2005). Data symbols are categories according to their HCA clusters (see. Figure 6).

Ca^{2+} + Mg^{2+} show a good correlation with HCO_3^- for both the rainy season (Figure 10) and dry season (Figure 10), indicating a possible dissolution of carbonates (Table 3). The equivalent ratio between (Ca^{2+} + Mg^{2+}) and HCO_3^- should be close to 1 and 2 if carbonate minerals are dissolved only by carbonic acid (Table 3) and if carbonate dissolution is coupled to sulphide (e.g., pyrite) oxidation (Table 3), respectively. In Figure 10, most of samples from the dry season and samples in C2 (both seasons) scatter between the 2:1 line and 1:1 line, indicating that both carbonic acid and sulphide oxidation contribute protons for carbonate dissolution processes. In addition, in the dry season, the excess amount of Ca^{2+} + Mg^{2+} over HCO_3^- ions (Figure 10) is almost compensated by SO_4^{2-} ions and the

samples plot around the 1:1 line between (Ca^{2+} + Mg^{2+}) and (HCO_3^- + SO_4^{2-}) (Figure 10). Further, the total cations plot around the 2:1 line with HCO_3^- (Figure 11) and HCO_3^- + SO_4^{2-} (Figure 11). Moreover, total cations adjusted for effect of evaporation and evaporite dissolution (Cl^-) and silicate weathering (Si) are almost balance by HCO_3^- + SO_4^{2-} (Figure 11), showing the effect of carbonate dissolution by carbonic acid (Figure 11) and coupled with sulphide oxidation (Figure 11).

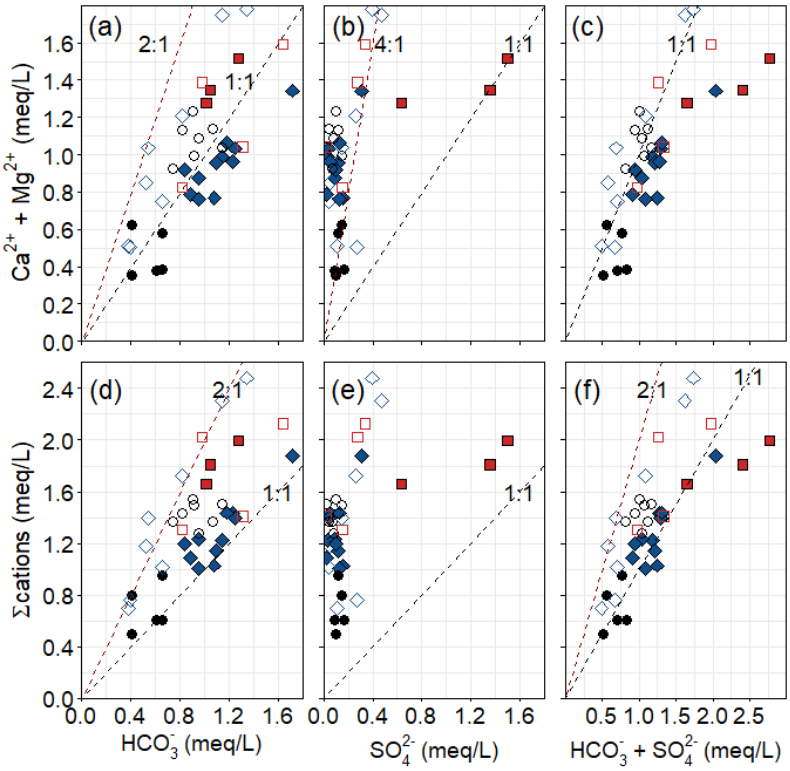

Figure 10: Bivariate plots showing variation of Ca^{2+} + Mg^{2+} and total cations with HCO_3^- , SO_4^{2-} and the sum of HCO_3^- and SO_4^{2-}). Data symbols are categories according to their HCA clusters (see. Figure 6), with open symbols for the dry season.

-

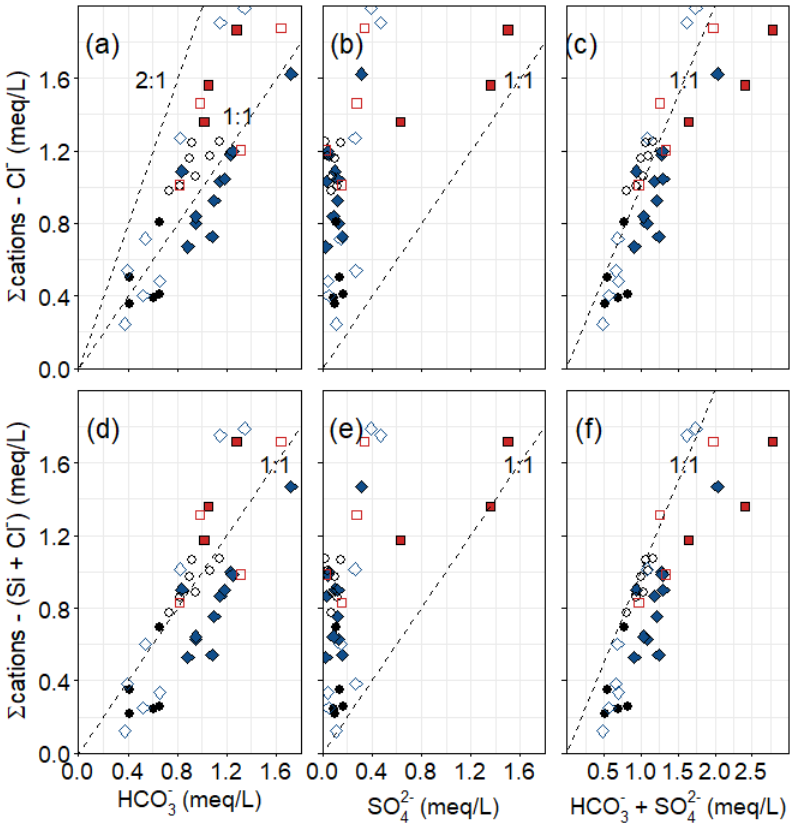

Figure 11: Bivariate plots showing variation of total cations corrected for effect of evaporation and dissolution of evaporites and silicates with HCO_3^-, SO_4^{2-} and the sum of HCO_3^- and SO_4^{2-}). Data symbols are categories according to their HCA clusters (see. Figure 6), with open symbols for the dry season.

However, many of the rainy season samples have ratios of (Ca^{2+} + Mg^{2+}): HCO_3^- (Figure 10) and (Ca^{2+} + Mg^{2+}): (HCO_3^- + SO_4^{2-}) (Figure 10) that are <1:1 and the dry season samples plot below the 2:1 line (Figure 10). The excess HCO_3^- in these waters is balanced by Na^+ + K^+ for the rainy season (Figure 10 and Figure 11). Further, the total cations plot around the 1:1 line with HCO_3^- (Figure *10*) and HCO_3^- + SO_4^{2-} (Figure *10*). Moreover, total cations adjusted for effect of evaporation and evaporite dissolution (Cl^-) and silicate weathering (Si) are not balanced by HCO_3^- + SO_4^{2-} (Figure *11*). In this environment, the principal sources of Na^+, K^+, and Si are silicate minerals (Bhatia *et al*., 2013; Wadham *et al.* 2010). Additionally, the river waters show low, but variable, molar (Ca^{2+}+Mg^{2+})/(Na^++K^+) ratios (Figure *10*) suggesting the importance of the silicate

reactions and the high variation in the relative intensity of silicate and carbonate weathering.

This is consistent with chemical weathering reactions involving mainly carbonic acid, and protons from sulphide oxidation, releasing Na^+ and K^+ cations from silicates and Ca^{2+} and Mg^{2+} from silicates and carbonates. This conclusion is also supported by the presence of significant positive correlations between the major cations (Na^+, K^+, Ca^{2+}, Mg^{2+}) and with Si and HCO_3^- (Figure *7*). These variations are also represented by PC1 and therefore explain the highest variation in the dataset. However, the observed SO_4^{2-}/HCO_3^- molar ratios in the river water are generally low. In addition, $Na^+ + K^+$ contents are poorly correlated with SO_4^{2-} (R = 0.37), suggesting a minor importance of sulphide oxidation reactions (Table 1). Figure 9 show that this true for most of the rainy season samples, with the importance of sulphuric acid weathering being recognised more in the dry season samples and in the rainy season for C2 samples. The rainy season C2 samples have high SO_4^{2-}/HCO_3^- molar ratios close to 1 and sulphate mole fractions (SMF) of 0.4 and $(Ca^{2+} + Mg^{2+})/SO_4^{2-}$ molar ratio of 1 (Figure *10*). Further, the analysis above shows that silicate dissolution seems more important in the rainy season than the dry season. This is attributed to higher runoff in the rainy season, whereas in the dry season most of the flow contribution is from groundwater (Figure *12*). Over the study area, the annual calculated baseflow is in the order of 6 Mm^3 per annum over the 156 km^2 catchment area (Figure *12*). For the North Rukuru (at Mwakimene station), the daily average baseflow index (BFI) was about 71% (Figure 12). The mixing with groundwater and evapo-concentration leads to higher levels of major ions, notably Na^+ and Cl^- (Figure *5*) in the dry season than rainy season.

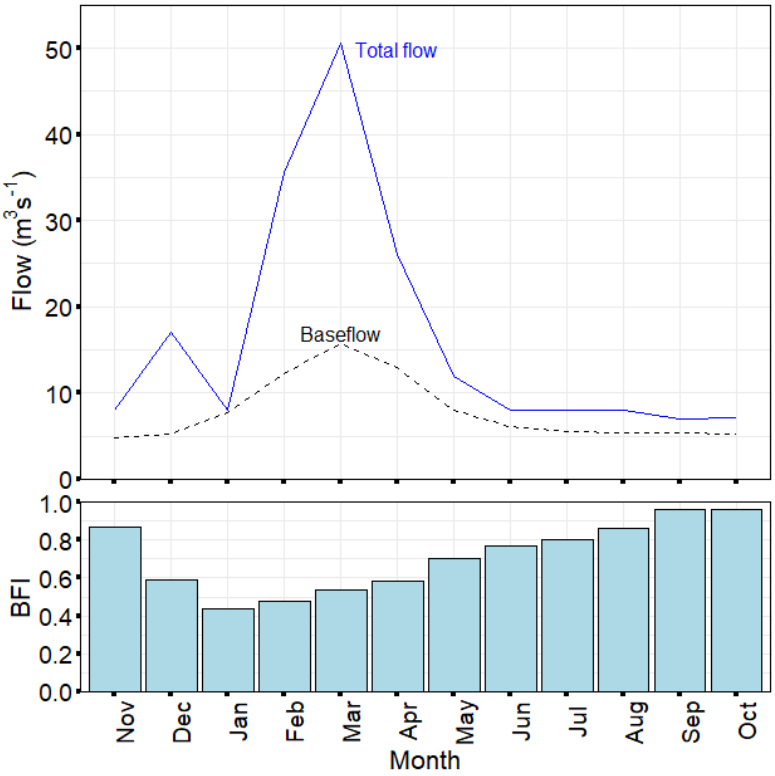

Figure 12: Total flow, baseflow and baseflow index (BFI) for the North Rukuru River at Mwakimene. The daily baseflows were calculated in R using Hydrostat package.

In the study area, the main silicate materials include feldspars (microcline, albite, and plagioclase), muscovite, biotite, hornblende, quartz, chlorite, illite, kaolinite and smectite. In addition, calcite, haematite, and carbonaceous material associated with pyrite are also present (Atkins, 1990; Carter & Bennet, 1973; Ray, 1975; Shluter, 1997). The oxidised arkoses show feldspar deterioration and prevalence of primary hematitic matrix partially altered to geothite/limonite on weathering, whereas the reduced arkoses contain fresh feldspars and carbonaceous debris with pyrite and chlorite. The oxidized arkoses are found at or near the surface, where dominant kaolinite is also present, and thus probably relate to relatively recent weathering.

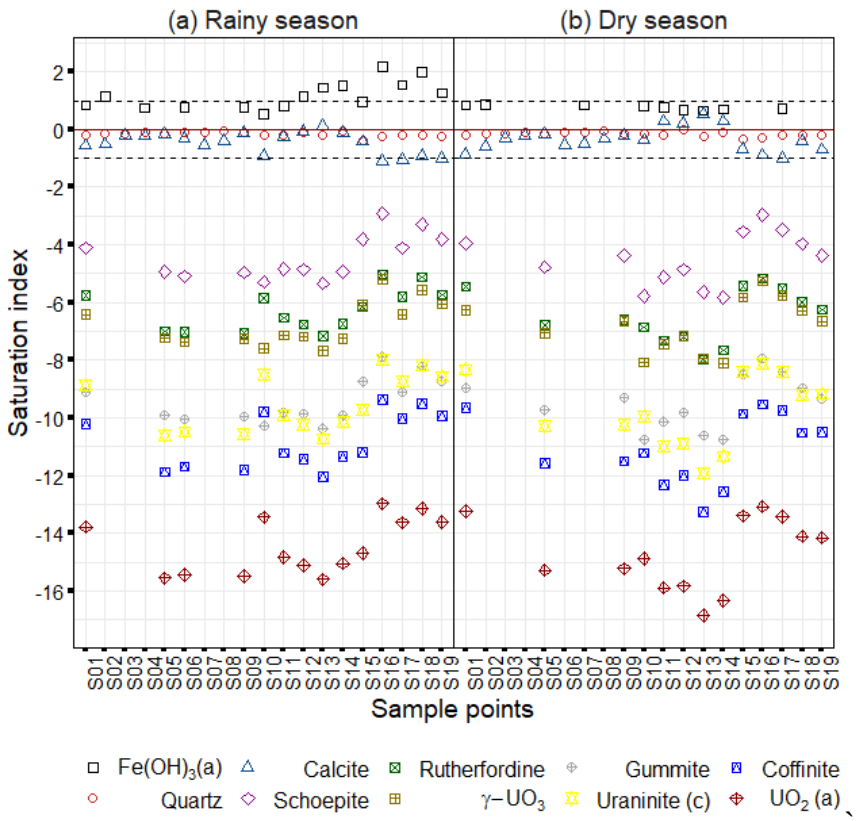

Figure 13: Saturation Indices of selected mineral phases calculated using PHREEQC v3 (Parkhurst and Appelo, 2013)

In Figure 9, the river waters plot in the kaolinite stability field and show remarkable relative constancy in silica activity, indicating short reaction paths and well-drained conditions (Appelo & Postma, 2005; Drever, 1997), which is reflected in the generally low levels of dissolved salts. Basement rocks, particularly gneisses, are typically resistant to erosion and dissolution whereas the soluble salts within sedimentary deposits of the Karoo are generally more susceptible to dissolution, particularly the arkose deposits (Atkins, 1990). In addition, generally, the samples show saturation to slight supersaturation with quartz, iron (III) oxyhydroxides and calcite, but undersaturated with respect to many uranium compounds (`

Figure 13). Therefore, sodium may be derived from albite and plagioclase weathering to kaolinite (Figure 9), whereas alteration of K-feldspar, muscovite and biotite to kaolinite may constitute the probable source of K^+. Dissolved Ca and Mg may have multiple mineral

sources in the studied waters (e.g., plagioclase, biotite, carbonates). Although plagioclase is a compositional solid solution between anorthite ($CaAl_2Si_2O_8$) and albite ($NaAlSi_3O_8$), the variation in composition does not affect the ratio (in equivalents) of the product cation to either the HCO_3^- or the SO_4^{2-} produced (cf. Eqs. (5a), (5b), (6a) and (6b)). In addition to mineral weathering, the oxidation of organic matter will produce HCO_3^- (Table *3*,Eq. (9)), which is expected to occur in the dambos in the catchments. On the other hand, sulphates and (sulphuric acid) may be generated by natural oxidation of disseminated pyrite (and consequent precipitation of Fe (III) oxides/oxyhydroxides) (Eqs. (4a). This is supported by the levels of sulphate in the water (up to 470 µeq/L), as expected from oxidation of pyrites by oxygen saturated water.

PHREEQC v3 (Parkhurst and Appelo, 2013) was used to account for observed changes in water chemistry along river flow, within the identified principal groups of surface water (based on hierarchical cluster analysis). The first approach evaluated the extent to which chemical equilibria among the major present minerals and surface water represents the river water chemistry. In this way, PHREEQC calculated the solution composition following successive addition of small amounts of the identified minerals (Table 4) to pure water and the system was allowed to achieve chemical equilibrium between each addition (Appendix 1). The chemical changes along the incrementally calculated reaction path are best displayed om the stability diagram (Figure 9). The solution composition follows a path resembling a natural system saturated with CO_2, which decreasing the pH rise associated with the K-mica and K-feldspar weathering (Drever, 1997), but in which quartz doesn't dissolve i.e., the amount of silica is controlled by quartz solubility (Figure 9).

Table 3: Equations describing the principal geochemical weathering reactions

A. **Carbonate and silicate dissolution with carbonic acid**

(1) *Carbonate dissolution*

$Ca_{1-x}Mg_xCO_3$ (s) + CO_2 (aq) + H_2O (l) → (1-x) Ca^{2+}(aq) + xMg^{2+} (aq) + $2HCO_3^-$ (aq)

(2) *Alteration of biotite to kaolinite*

$2KMg_3AlSi_3O_{10}(OH)_2$(s) + $14CO_2$ (aq) + $7H_2O$(l) →$Al_2Si_2O_5(OH)_4$ (s) + $6Mg^{2+}$(aq) + $2K^+$ (aq) + $14HCO_3^-$(aq) + $4SiO_2$(aq)

(3) *Alteration of plagioclase to kaolinite*

$38Na_{0.62}Ca_{0.38}Al_{1.38}Si_{2.62}O_8$ (s) + $52CO_2$ (aq) + $78H_2O$ (l) → $26Al_2Si_2O_5(OH)_4$ (s) + $24Na^+$(aq) + $14Ca^{2+}$(aq) + 52 HCO_3^- (aq) + 47 SiO_2 (aq)

(4) *Alteration of K-feldspar to kaolinite*

$2KAlSi_3O_8$ (s) + $2CO_2$ (aq) + $3H_2O$ (l) → $2K^+$ (aq) + $2HCO_3^-$ (aq) + $Al_2Si_2O_5(OH)_4$ (s) + $4SiO_2$ (aq)

B. Sulphide oxidation coupled to carbonate and silicate dissolution

(5) *Carbonate dissolution*

$16Ca_{1-x}Mg_xCO_3$ (s) + $4FeS_2$ (s) + $15O_2$ (aq) + $14H_2O$ (l) →$16(1-x)$ Ca^{2+}(aq) + $16xMg^{2+}$ (aq) + $16HCO_3^-$ (aq) + $8SO_4^{2-}$ (aq) + $4Fe(OH)_3$(s)

(6) *Alteration of biotite to kaolinite*

(6) $2KMg_3AlSi_3O_{10}(OH)_2$ + $2FeS_2$ (aq) + $6O_2$ (aq) + $3H_2O$ → $2K^+$ + 6 Mg^{2+} + $4SO_4^{2-}$ + $Al_2Si_2O_5(OH)_4$ (s) + $4SiO_2$ (aq) + $2Fe(OH)_3$ (s)

(7) *Alteration of plagioclase to kaolinite*

$Na_{0.62}Ca_{0.38}Al_{1.38}Si_{2.62}O_8$ (s) + FeS_2 (aq) + $3.5O_2$ (aq) + $4.61H_2O$ (l) → $0.69Al_2Si_2O_5(OH)_4$ (s) + $0.62Na^+$(aq) + $0.38Ca^{2+}$(aq) + $2SO_4^{2-}$ (aq) + $Fe(OH)_3$ (s) + $1.24SiO_2$ (aq)

(8) *Alteration of K-feldspar to kaolinite*

$8KAlSi_3O_8$ (s) + $4FeS_2$ (aq) + $17O_2$ (aq) + $14H_2O$ (l) → $8K^+$ (aq) + $8SO_4^{2-}$ (aq) + $4Al_2Si_2O_5(OH)_4$ (s) + $4Fe(OH)_3$ (s) + $16SiO_2$ (aq)

(9) Oxidation of organic matter

$CH_2O + O_2 \rightarrow CO_2 + H_2O \rightleftharpoons HCO_3^- + H^+$

In the second approach, inverse modelling was used to find sets of minerals and gases that, when reacted in appropriate amounts, account for the differences in composition between two endmembers (Table 4) along the flow path in each cluster (Lecomte *et al*., 2005). The models were formulated so that primary mineral phases reported to be present, such as biotite, feldspars, pyrite, plagioclase, and calcite were constrained to dissolve until they reached saturation, whereas secondary clay minerals such as kaolinite and quartz were set to precipitate once they reached saturation. Carbon dioxide and oxygen were assumed to be available throughout the flow path. Representative results of the inverse geochemical modelling are summarised in Table *4*. The models were selected based on statistics reported by PHREEQC (sum of residuals and maximum fractional error) and size of mole transfers for mineral phases (>1 mol considered are not realistic) (e.g., Rosenthal *et al.*, 2007). The selected models corroborate that the main reactions are dissolution of calcite, plagioclase, biotite, feldspars with carbon dioxide and pyrite consumption; kaolinite, iron (III) hydroxides and quartz precipitate in different amounts (Table *4*). The contribution of pyrite oxidation is shown to be higher in the middle section of the Sere River than in the upper reaches of the study area. In addition, there's a dilution effect (simulated as addition of water phase) mainly in the rainy season and in the North Rukuru River, attributed to high recharge and discharge, respectively.

Table 4: Summary of results of inverse modelling with PHREEQC

Phases	Phase mole transfers (mol)					
	S03-S09		S11-S14		S16-S19	
Dry season						
Kaolinite	-0.000314	-0.000186	-0.000036	-0.000074	-0.000065	-0.000134
Calcite	-0.000282	-0.000154	0.000113	0.000074	0.000122	0.000053
Fe $(OH)_3$ (a)	-0.000018	-0.000018	-0.000030	-0.000030	0.000000	0.000000
Pyrite	0.000018	0.000018	0.000030	0.000030	0.000000	0.000000
K-feldspar	0.000000	0.000000	0.000000	0.000000	0.000004	0.000004
CO_2 (g)	0.000128	0.000000	0.000260	0.000298	0.000192	0.000261
O_2 (g)	0.000042	0.000042	0.000113	0.000113	0.000000	0.000000
Albite	0.000000	0.000209	0.000063	0.000000	0.000113	0.000000
Biotite	0.000006	0.000006	0.000008	0.000008	0.000013	0.000013
Quartz	-0.000565	-0.000565	-0.000121	-0.000121	-0.000220	-0.000220
Plagioclase	0.000451	0.000113	0.000000	0.000102	0.000000	0.000182
H_2O	0.00	0.00	0.00	0.00	23.73	23.73
Rainy season						
Kaolinite	-0.000091	-0.000154	-0.000166	-0.000317	-0.000022	-0.000030
Calcite	0.000122	0.000059	0.000307	0.000156	0.000062	0.000048
Fe $(OH)_3$(a)	-0.000009	-0.000009	-0.000254	-0.000254	-0.000024	-0.000024
Pyrite	0.000010	0.000010	0.000255	0.000255	0.000021	0.000020
K-feldspar	0.000064	0.000064	0.000024	0.000024	0.000012	0.000012
CO_2 (g)	0.000126	0.000188	0.000097	0.000248	0.000000	0.000000
O_2 (g)	0.000145	0.000145	0.001048	0.001048	0.000108	0.000097
Albite	0.000101	0.000000	0.000246	0.000000	0.000021	0.000000
Biotite	0.000018	0.000018	0.000062	0.000062	0.000011	0.000010
Quartz	-0.000321	-0.000321	-0.000610	-0.000610	-0.000073	-0.000065
Plagioclase	0.000000	0.000164	0.000000	0.000397	0.000000	0.000028
H_2O	26.59	26.59	25.69	25.69	7.23	5.25

4.2.2. Anthropogenic processes

Samples collected from North Rukuru River (S16-S19) in cluster 1 and sample 9 from cluster 3 show significantly elevated levels of nitrates in the rainy season compared to the dry season (Figure *5*). In general, samples in cluster 1 have relatively lower mineralisation than other samples attributable to dilution from higher discharge of the North Rukuru River. In the studied area, nitrates in surface water are negatively correlated to sodium (Figure *7*). Therefore, while dilution lowers the concentrations of all dissolved solutes, decrease in nitrate levels is compensated with input along the course of the North Rukuru.

On the other hand, samples in cluster 2 (Sere River), show relatively higher levels of sulphate than other samples and sulphate levels are remarkably more elevated in the rainy season over the dry season levels (Figure *5*). Hence, the results show that there are other sources of NO_3^- and SO_4^{2-} in the study area. In general, high NO_3^-/Na^+ and NO_3^-/Cl^- ratios are associated with agricultural inputs because organic/inorganic fertilisers are generally rich in NO_3^-, with low Na^+ and Cl^- contents (Figure *14*), while NO_3^- originating from human excreta, animal wastes and septic effluents has a strong correlation with Cl^- (Anornu *et al*., 2017; Liu *et al*., 2006). The high values of NO_3^-/Na^+ appear in S19, S18, S16 (Figure *14*), draining a typical agricultural zone.

On the other hand, the elevated SO_4^{2-} levels and high SO_4^{2-}/Cl^- molar ratios indicate a point source associated with anthropogenic activities (Figure *14*). Samples in cluster 2 (Sere River) were taken in an area below Tailings Storage Facility A (TSF A) (Figure *3*). At Kayelekera, the extraction of uranium from ores involved leaching with sulphuric acid. The effluent and tailings from the mill were then discharged as a slurry to a waste-retention pond and protected by a water cover. Composition of uranium mill tailings depends on the original ore material and comprises primary gangue and secondary minerals (Abdelouas, 2006). In the present case, the primary minerals include quartz, feldspars, plagioclases, micas (biotite and muscovite), clay minerals (smectite, kaolinite and illite and chorite), along with hematite, pyrite, carbonaceous debris, and calcite. The secondary minerals are those formed by the precipitation of ore species and reagents added during processing and neutralization and include iron oxyhydroxides, gypsum and uranyl sulphates (e.g., jarosite, zippeite) (Abdelouas, 2006).

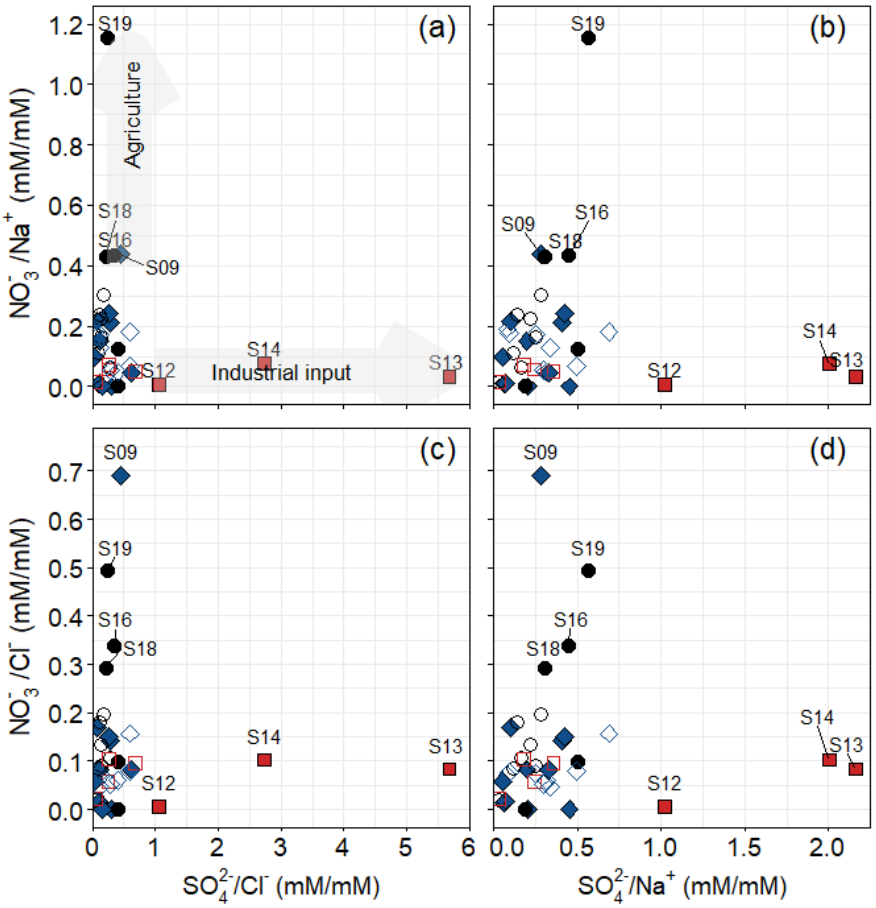

Figure 14: Relationship between NO_3^-/Na^+ and NO_3^-/Cl^- with SO_4^{2-}/Na^+ and SO_4^{2-}/Cl^- for both the rainy and dry seasons. Data symbols are categories according to their HCA clusters (see.), with open symbols for the dry season.

In the rainy season, the elevated sulphate and TDS levels in these samples are accompanied by elevated levels of potassium (Figure 5). In addition, they show equivalent ratios (Ca^{2+}+ Mg^{2+}) and HCO_3^- to SO_4^{2-} of around 1. This is consistent with bicarbonate and silicate weathering coupled by oxidation of pyrite (Table 1). Seepage from the tailing's impoundment and/or spills may be a probable source of contaminant loads directly into receiving river or through infiltrating into the subsurface, respectively. Infiltrating water provides both oxygen and water (Kalin *et al*., 1992) for oxidation of sulphide minerals in the tailings. Even when the effluents are transferred to containment pools for evaporation, the risk of spills remain (Lottermoser & Ashley, 2005). At Kayelekera mine, various spills have been reported, for example in March 2013 and January 2015. Around TSF A, the

overall groundwater flow direction is towards Sere River (gradient 1 to 2%), but locally towards the Kantchindu Stream which flows through the valley across TSF A towards Sere River (Figure *3*). Groundwater levels are generally shallow along the valley floor, appearing in some areas along the stream channel, and in the basement rock near the stream (2-3 m below surface). Although groundwater levels are generally deeper along the valley slopes (10-20 m below surface), perched conditions do occur, especially in the Karoo sediments (Atkins, 1990). From an environmental perspective, Uranium mine tailings do not represent an element of concern as released uranium could be immobilized by the newly formed secondary minerals such as oxyhydroxides. A seepage detection dam has been built in the Kantchindu valley downstream of the main tailings dam to intercept any seepage that may leak through the basin lining and grout curtain (EIA report, 2006).

4.3. Geochemical controls of uranium in water

The distribution of uranium species in water is dependent on temperature, pH, Eh and abundance of ligands such as calcium and bicarbonate ions (Davis *et al.*, 1998; Payne and Waite, 1991). Complexation with these ligands plays a significant role in the mobilization of oxidized uranium (VI) from the soil and sedimentary matrices (Wazne *et al*., 2003; Zheng *et al.*, 2003). In the pH range of river water samples (7.28 to 8.83), the dominant U(VI) species included $Ca_2UO_2(CO_3)_3$ and $UO_2(CO_3)_2^{2-}$, with minor amounts of $CaUO_2(CO_3)_3^{2-}$(Figure 15). In addition, $(UO_2)_2CO_3(OH)_3^-$ mainly exists in the samples from lower reaches of the study area along North Rukuru River clustered in C1 (Figure *2*). This is related to U speciation changes induced primarily by variations in Ca^{2+} and HCO_3^- concentrations and consumption of oxidized species (e.g., DO and Fe^{3+}), under oxidizing and alkaline conditions. The formation of calcium-uranyl-carbonate complexes e.g., $Ca_2UO_2(CO_3)_3$, is attributed to presence of Ca^{2+} from dissolution of plagioclase and carbonates. Whereas dilution due to high discharge of the Rukuru River, leads to formation of $(UO_2)_2CO_3(OH)_3^-$.

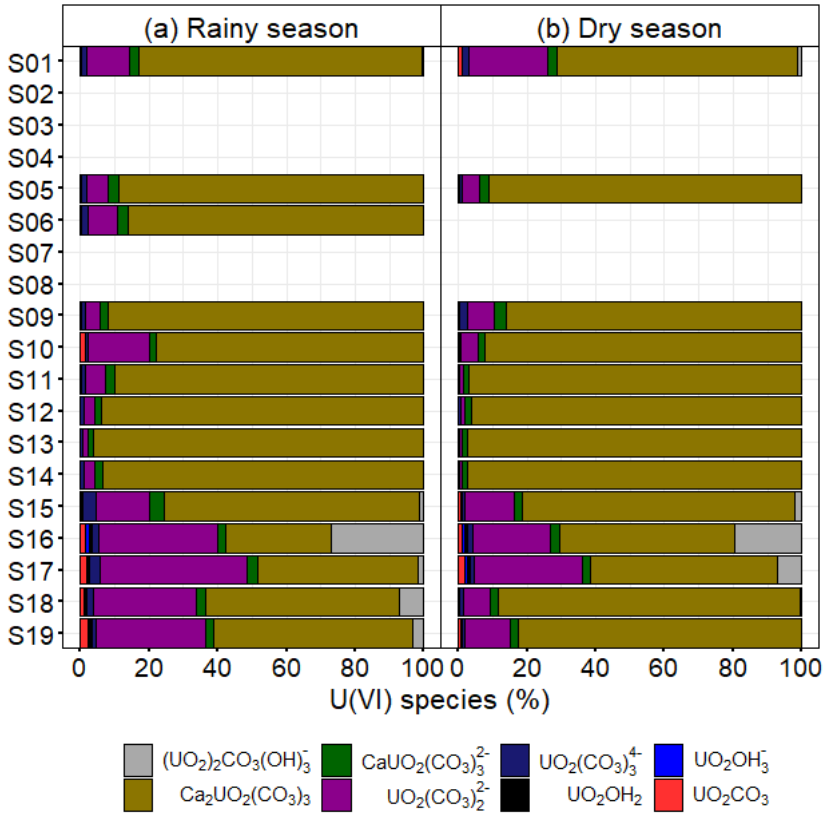

Figure 15: Distribution of uranium species in river water samples for both rainy and dry seasons. The samples are identified by their sample numbers and samples in which uranium was not detected are shown as blank.

Higher U concentrations were accompanied by higher pH values (dry season) and higher Fe (rainy season), sulphate and chloride concentrations (dry season), but by lower Eh values and Si, and HCO_3^- concentrations (Figure *5*). The levels of uranium in water are affected by adsorption onto organic matter and minerals such as ferrihydrite, goethite, hematite, and quartz (Fox *et al*., 2006; Guo *et al*., 2009; Murphy *et al*., 1999) and precipitation of secondary uranium minerals (Davis *et al.*, 2000). However, calcium-uranyl-carbonate complexes poorly adsorb (Stewart *et al*., 2010; Wazne *et al*., 2003; Zheng *et al*., 2003), hence their formation increases uranium mobility. The correlation between U and Fe may suggest U(IV) oxidation by Fe $(OH)_3$ (Ginder-Vogel *et al*., 2006, 2010), which may be microbially mediated. Naturally, uranium appears in tetravalent state and the more soluble hexavalent state. Ferric ions are known to play an important role in the oxidation of U(IV) under ambient conditions of temperature and pressure. In the

sedimentary environment (e.g., in mudstones and shales), primary U minerals are disseminated with pyrite and organic matter (OM). High OM contents may facilitate Fe (III)-and sulphate-reducing bacteria activities. On the other hand, the negative correlation with Si may suggest adsorption on detrital quartz or feldspar grains or in the matrix of secondary silicates such as illite or chlorite (Wilde *et al.*, 2019).

In summary, a conceptual model for the geochemical control of uranium in the river water is proposed. The oxidised rainwater (recharge and run off in the rainy season) and river water favours oxidation of pyrite and precipitation of iron oxyhydroxides. This, in turn, leads to oxidation of U(IV)-bearing minerals (e.g., UO_2, $U(SiO_4)$. nH_2O) releasing U(VI) species to water (surface and groundwater) and subsequently, complexation of UO_2^{2+} with CO_3^{2-} and Ca^{2+}, and retention of these U(VI) species by iron hydroxides and quartz grains. The Ca-UO_2-CO_3 complexes contribute to U mobility as they suppress adsorption (Brooks *et al.*, 2003; Neiss *et al*., 2007; Stewart *et al*., 2010; Zhang *et al*., 2015). The subsequent U(VI) desorption due to the formation of Ca–UO_2–CO_3 complexes relies on the specific adsorbed species ($Ca_2UO_2(CO_3)_3$, $CaUO_2(CO3)_3^{2-}$, $UO_2(CO_3)_2^{2-}$, $UO_2(CO_3)_3^{4-}$, or $(UO_2)_2CO_3(OH)_3^{-}$) leading to spatial variation in U concentrations (Wu et al., 2018).

CHAPTER 5

CONCLUSION AND RECOMMENDATION

5.1. Conclusion

Water samples collected from North Rukuru River and its surrounding rivers in 2018 and 2019 were analysed using chemical molar ratio, hierarchical, principal component analysis, and geochemical modelling. The chemical composition of the Sere River water composition was characterised by Ca-HCO_3^- in the dry season and Ca-HCO_3^--SO_4^{2-} in the rainy season, Chapwasha River, Mapambo River, Luwembe River and Muswanga River were explained by Ca-Mg- HCO_3^- composition in both seasons. North Rukuru river water was described by a mixed cation-HCO_3^- composition in the rainy season, which changes to mixed cation- HCO_3^--Cl^- composition in the dry season. Ca^{2+}, Mg^{2+} and HCO_3^{3-} were mainly provided from carbonate weathering while Na^+ and K^+ originated from silicate weathering. H_2CO_3 and H_2SO_4 make a significant contribution to the weathering process, with the importance of sulphuric acid weathering being recognised more in the dry season samples and in the rainy season for Sere River samples. The study showed that the main reactions are dissolution of calcite, plagioclase, biotite, feldspars with carbon dioxide and pyrite consumption; kaolinite, iron (III) hydroxides and quartz. Further, North Rukuru and Sere River water samples were affected by anthropogenic activities from agricultural inputs and mining activities. Agricultural activities resulted in an increase in nitrate levels in the North Rukuru while mining activities resulted in an increase in sulphate level in Sere River. The study revealed the dominant U(VI) species as $Ca_2UO_2(CO_3)_3$ and $UO_2(CO_3)_2^{2-}$.

In addition, $(UO_2)_2CO_3(OH)_3^-$ mainly exists in the samples from lower reaches of the study area along North Rukuru River. All samples were found within the WHO drinking water guild line standard except pH and Fe in both seasons and rainy season respectively.

3.4 5.2. Recommendation

This study proposes a conceptual model for the geochemical control of uranium in the river water of the study areas. In addition, groundwater and surface water interaction should be studied in the study area.

REFERENCES

Abdelouas, A. (2006). Uranium mill tailings: geochemistry, mineralogy, and environmental impact. *Elements,* 2, 335–341.

Alam, M. J. B., Islam, M. R., Muyen, Z., Mamun, M., & Islam, S. (2007). Water quality parameters along rivers. International Journal of Environmental Science & Technology, 4(1), 159–167. https://doi:10.1007/bf03325974.

Alam, M. J., et al. (2007) Water Quality Parameters along Rivers. International Journal of Environmental Science & Technology, 4, 159-167. https://doi.org/10.1007/BF03325974.

Alberto W. D., Maria de Pilar, D.A., Maria Valeria A., Fabicuaps, Cecillia H.A. & Moric de los Angeles. B. (2001). Pattern recognition techniques for evaluation of spatial and temporal variations in water quality. A case studies. Suqua river Basin. *Cordoba, -Argentina- water research,* 35, 2881-2894.

Al-Zarah, A. l. (2007). Hydrogeochemical processes of alkhobar aquifer in Eastern region, Saudi Arabia. *Journal of Applied Science*, 7:3669-3677.

American Public Health Association (APHA). (1992). *Standard Methods for the Examination of Water and Wastewater, 18th Edition*. Washington D.C.

Amfo-out, R, Agyenim J.B., & Nimba-Bumbah, G. B. (2014). Correlation analysis of ground water colouration from mountainous areas, Ghana. *Environ. Res. Eng. Manage*. 67:16-24.

Anon. (1992). *Standard Methods for the Examination of Water and Wastewater (18thed).* Washington D.C. USA. APHA/AWWA/WPCF.

Anon. (1993). *Guideline for drinking water quality.* World Health Organization. Geneva.

Anornu, G., Gibrilla, A., & Adomako, D. (2017). Tracking nitrate sources in groundwater and associated health risk for rural communities in the White Volta River Basin of Ghana

Appelo & Postma. (2003). *Principles and application of geochemistry*. A comprehensive textbook for Geology student. New jersey, prentice -Hall.

Appelo, C.A.J. & Postma (1993). *Groundwater and pollution*. Rotterdam, Netherlands: A.A. balkema

Appelo, C.A.J., & Postma. D. (2005). *Geochemistry, Groundwater, and pollution*. Amsterdam, A.A. Balkema publishers.

Arain, M. B, Kazi, T. G., Jamali, M. K., Jalbani, N., Afridi, H.I., & Shah, A. (2008). Total dissolved and bioavailable elements in water and sediment samples and their accumulation in Oreochromis mossambicus of polluted Manchar Lake. *Chemosphere* 70:1845–1856

Atkins, 1990, Kayelekera Uranium Project Environmental Assessment. Report prepared by W S Atkins Environmental for the Central Electricity Board of Great Britain, United Kingdom. (As cited by KEIA).

Back, W., & Hanshaw, B.B. (1971). *Chemical geohydrology*. Advances in Hydro science, Academic Press, New York, Vol. 2, pp.49–104, 1965.S Carolina.

Barakat, A., El Baghdadi, M., Rais, J., & Nadem, S. (2016). Assessment of spatial and seasonal water quality variation of Oum Er Rbia River (Morocco) using multivariate statistical techniques. *International Soil and Water Conservation Research*, 4(2016), 284–292.

Bowden, R.A., & Shaw, R.P. (2007). The Kayelekera uranium deposit, Northern Malawi: past exploration activities, economic geology and decay series disequilibrium, *Applied Earth Sci.* (Trans. Inst. Min. Metall. B) 116 ,55–67.

Bricker, O.P., & Jones, B.F. (1995). Main factors affecting the composition of natural waters. In: Salbu, B., Steinnes, E. (Eds.), *Trace Elements in Natural Waters*. CRC Press, Boca Raton, FL, pp. 1e5.

British Geological Survey (2009) Malawi Potential of Malawi. Malawi Government, Malawi.

Buck, O., Niyogi, D. K., & Townsend, C. R. (2004). Scale-dependence of land use effects on water quality of streams in agricultural catchments. Environmental Pollution, 130(2), 287–299. https://doi:10.1016/j.envpol.2003.10.018.

Carroll J., Savinov V., Savinova T., Dahle S., McCrea R., & Muir D. C. G. (2008). PCBs, PBDEs and pesticides released to the Arctic Ocean by the Russian Rivers Ob and Yenisei. *Environ. Sci. Technol.*, 42 (1), 69–74, 10.1021/es071673l.

Carter G.C., Bennet L.H., Cahan D.J. (1977) Metallic Shifts in NMR, Prog. in Material Sci. Vol. 20, Pergamon Press, London

Chadha, D.K. (1999). A proposed new diagram for geochemical classification of natural water and interpretation of chemical data. *Hydrogeology Journal.*, 7(5). 431-439.

Chang, H. (2008). Spatial analysis of water quality trends in the Han River basin, South Korea. *Water Research*, 42, 3285-3304.

Charete, M.A., & Sholkovitz. E. R. (2002). Oxidative precipitation for groundwater derived ferrous iron in subterranean estuary of a coastal bay. *Geophysical Research Letters*, 29(10): 1-4.

Charkhabi, A.H. & Sakizadeh, M., (2006). Assessment of Spatial Variation of Water Quality Parameters in the Most Polluted Branch of the Anzali Wetland, Northern Iran, 15(3), 395–403.

Chauban, A. & Singh, S., (2004). Evaluation of Ganga Water for Drinking Purpose. *By Water Quality Index at Rishikesh*, Uttarakhand, India

Cloutier, V. Lefebre R., & Therren. R. (2008). Multivariate statistical analysis of geochemical data as an indicative of hydrogeochemical evolution of groundwater in sedimentary rock aquifer system. *Journal of hydrology*, 353(3-4), 294-313. http://dx.doi.org/10.1016/j.hydrol.2008.02.15.

Courage D. E., ·Geophrey, A., · Emmanuel, K., & Samuel, Y. (2018). Evaluation of water quality using hydrochemistry, stable isotopes, and water quality indices in the Lower Volta River Basin of Ghana. *Environ Dev Sustain*. https://doi.org/10.1007/s10668-018-0180-5

Cruz J. V., & Amaral C. S. (2004). Major ion chemistry of groundwater from perched-water bodies of the Azores (Portugal) volcanic archipelago," *Applied Geochemistry*, vol. 19, no. 3, pp. 445–459, 2004.

Dallas, H.F., & Jay, J.A. (2004). The effect of water quality determination aquatic ecosystems. *Water Research commission*. A review. Report number: 224/04.

Davis J. A; David E. Meece; Matthias Kohler; Gary P. Curtis (2004). Approaches to surface complexation modeling of Uranium (VI) adsorption on aquifer sediments., 68(18), 0–3641. doi: 10.1016/j.gca.2004.03.003

Deutsche, W.J. (1997). *Groundwater geochemistry*. Boca rato; CRC press.

Ding, J., Jiang, Y., Fu, L., Liu, Q., Peng, Q., & Kang, M. (2015). Impacts of Land Use on Surface Water Quality in a Subtropical River Basin: A Case Study of the Dongjiang River Basin, Southeastern China. *Water*, 7(8), 4427–4445.

Drever, J. I. (1994) The effect of land plants on weathering rates of silicate minerals. Geochim. Cosmochim. Acta 58, 2325–2332

Edmunds, W. M., Shand, P., Hart, P., & Ward, R. S. The natural (baseline) quality of groundwater: a UK pilot study. *Science of the Total Environment*, vol. 310, no. 1-3, pp. 25-35, 2003.

Edmunds, W.M., & Smedley, P.L. (2000). Residence time indicators in groundwater: The East Midlands Triassic sandstone aquifer. *Applied Geochemistry* 15, pp 737-752

Elango, L. (1992). Hydro geochemistry and modelling of multilayer aquifers. Ph.D. Thesis, *Anna University*, Chennai, India.

Elango, L., Kannan, R., & Senthil Kumar, M. (2003). Major ion chemistry and identification of hydrogeochemical processes of groundwater in a part of Kancheepuram District, Tamil Nadu, India. *Environmental Geosciences*, Vol. 10, No. 4, pp.157-166, 2003.

Elango, L., Rajmohan, N., & Gnanasundar, D. (2004). Groundwater quality monitoring, in intensively cultivated regions of Tamil Nadu, India, *Electronic Journal of Environmental, Agricultural and Food Chemistry*, *5*,2248-2261.

Elshorbagy, A., & Ormsbee, L. (2006). Object-oriented modelling approach to surface water quality management. *Environmental Modelling and Software*, 21(5), 689–698.

Elubid, B. A., Huang, T. H., Ahmed, E., Zhao, J. M., Elhag, K., Abbass, W. M., & Babiker, M. (2019). Geospatial Distributions of Groundwater Quality in Gedaref State Using Geographic Information System (GIS) and Drinking Water Quality Index (DWQI). *International Journal of Environmental Research and Public Health*, 16(5), 731. https://doi.org/10.3390/ijerph16050731

Fataei. E. and Shiralipoor. S. “Evaluation of Surface Water Quality Using Cluster Analysis: A Case Study,” World Journal of Fish and Marine Sciences, Vol. 3, 2011, pp. 366-370.

Frank, E., & Harrell. (2021). Hmisc: Harrell Miscellaneous. R package version 4.6-0. https://CRAN.R-project.org/package=Hmisc

Freeze, R.A. & Cherry, J.A. (1979). *Ground Water Flow*. New Jersey, Prentice- Hall Inc., pp. 15-77, 1979.

Gaillardet, J., Dupré, B., Louvat, P., & Allègre, C.J. (1999). Global silicate weathering and CO consumption rates deduced from the chemistry of large rivers. Chemical Geology, 159, 3–30.

Gaillardet, J., Dupré, B., Louvat, P., & Allègre, C.J. (1999). Global silicate weathering and CO consumption rates deduced from the chemistry of large rivers. *Chemical Geology*, 159, 3–30

Galili, T. (2015). dendextend: an R package for visualizing, adjusting, and comparing trees of hierarchical clustering. Bioinformatics. https://doi.org/10.1093/bioinformatics/btv428

Galili, T. (2015). dendextend: an R package for visualizing, adjusting, and comparing trees of hierarchical clustering. Bioinformatics. https://doi.org/10.1093/bioinformatics/btv428

Gantidis, N., Pervolarakis, M. & Fytianos, K., (2007) Assessment of the quality characteristics of two lakes (Koronia and Volvi) of N. Greece. *Environ Monit Assess* 125:175–181

Gibbs, R.J. (1970). Mechanisms controlling world's water chemistry. *Science*, Vol. 170, pp. 1088-1090, 1970.

Ginder-Vogel, Matthew; Criddle, Craig S.; Fendorf, Scott (2006). Thermodynamic Constraints on the Oxidation of Biogenic UO ₂ by Fe(III) (Hydr)oxides. Environmental Science & Technology, 40(11), 3544–3550. doi:10.1021/es052305p

Guler, C.G., Thyne J. & Turner, K. (2002). Valuation of graphical multivariate statistical methods for classification of water chemistry data. *Hydrogeology/Geochemistry*, 10 (4). 455-474.

Hamdi-Aïssa, B., Vallès, V., Aventurier, A. & Ribolzi, O. Soils and brines geochemistry and mineralogy of hyper arid desert playa, Ouargla basin, Algerian Sahara. *Arid Land Res. Manage*., 18, 103–126, 2004.

Hem, J.D. (1992). *A study and interpretation of the chemical characteristics of natural water*. United States Geological Survey water supply paper. Washington, united states government printing office.

Hossain, A., (2001). Evaluation of Surface water Quality: A case study on Surma River, B.Sc. Engineering Thesis, Civil and Environmental Engineering Department, Shahjalal University,Bangladesh. http://www.epa.gov/compliance/resources/cases/civil/caa/ethanol/index.html

Hounslow, A.W. (1995). *Water Quality Data: Analysis and Interpretation*. CRC Press LLC, Lewis Publishers, Boca Raton.

Hudson, R.O., & Golding, D.L. (1997). Controls on groundwater chemistry in Subalpine catchments in the solution interior British Columbia. *Journal of Hydrology*, Vol. 201, pp. 1-20, 1997.

Hussain, M., Ahmed, S. M., & Abderrahman, W. (2008). Cluster analysis and quality assessment of logged water at an irrigation project, eastern Saudi Arabia. Journal of Environmental Management, 86(1), 297–307. https:// doi: 10.1016/j.jenvman.2006.12.007.

Hussain, M., Ahmed, S. M., & Abderrahman, W. (2008). Cluster analysis and quality assessment of logged water at an irrigation project, eastern Saudi Arabia. Journal of Environmental Management, 86(1), 297–307. https://doi:10.1016/j.jenvman.2006.12.007.

Jain, P., Sharma, J. D., Sohu, D., & Sharma, P. (2011). Chemical analysis of drinking water of villages of Sanganer Tehsil, Jaipur District. *Int. J. Environ. Sci. Tech.* Vol. 2, No. 4, pp. 373-379.

Jalali, M., (2010). Application of Multivariate analysis to study water chemistry of groundwater in asemi-arid aquifer, Malayer, Western Iran. *Desalination Water Treat. 19*, 307–317.

Jennings, G. D., & Seed, E. (1996). Nitrate in Drinking Water quality. Water quality and waste management. *Cooperative Extension Service*, AG 473-4. North

Jiang, Liguang; Yao, Zhijun; Wang, Rui; Liu, Zhaofei; Wang, Lei; Wu, Shanshan (2015). Hydrochemistry of the middle and upper reaches of the Yarlung Tsangpo River system: weathering processes and CO2consumption. Environmental Earth Sciences, 74(3), 2369–2379. https://doi:10.1007/s12665-015-4237-6.

Kaiser, H.F. (1958) The Varimax Criterion for Analytic Rotation in Factor Analysis. Psychometrika, 23,187-200. https://doi.org/10.1007/BF02289233

Kassambara, A. (2017). *Multivariate analysis I: Practical guide to cluster analysis in R.* sthda.com.

Kawo, N. S., & Karuppannan, S. (2018). Groundwater quality assessment using water quality index and GIS technique in Modjo River Basin, central Ethiopia. *Journal of African Earth Sciences*, 147(June), 300–311. https://doi.org/10.1016/j.jafrearsci.2018.06.034.

Kazi; M.B. Arain; M.K. Jamali; N. Jalbani; H.I. Afridi; R.A. Sarfraz; J.A. Baig; Abdul Q. Shah (2009). Assessment of water quality of polluted lake using multivariate statistical techniques: A case study. 72(2), 0–309. https://doi:10.1016/j.ecoenv.2008.02.024.

Kgabi N. (2015). Environmental Water Quality Processes Lecture Notes: Unit 1, Water Quality. *Polytechnic of Namibia, School of Engineering, and Department of Civil and Environmental Engineering*, Windhoek, Namibia

Kirby-Smith, W.W., & White, N. (2006). Bacterial contamination associated with estuarine shoreline development. *Journal of Applied Microbiology*. 100,648-657.

Kumar, M., & Puti, A. (2012). A review of permissible limits of drinking water. *Indian journal of occupational and environment medicine*, 16(1), pp.40-44.

Kumar, R.N., Solanki, R., & Kumar, N.J.I. (2011). An assessment of seasonal variation and water quality Index of Sabarmati River and Kharicut canal at Ahmedabad, Gujarat. https://www.researchgate.net/journal/Electronic-Journal-of-Environmental-Agricultural-and-Food-Chemistry-1579-4377

Kundzewicz, Z. W., Mata L.J., Arnell N.W., Döll, P., Kabat, P., Jiménez, B., Miller, K.A., Oki, T., & Shiklomanov, I.A. (2007). Freshwater resources and their management. In: Parry ML, Canziani, O. F., Palutikof, J.P., van der Linden, P.J., Hanson, C. E. (eds). Climate change 2007: *Impacts, Adaptation and Vulnerability. Contribution of Working Group II to the Fourth Assessment Report of the Intergovernmental Panel on Climate Change*, Cambridge University Press, Cambridge, pp 173–210

Langelier, W. F. (1946). Chemical Equilibria in Water Treatment. *Journal of American Water Works Association*, 38, 169.

Langmuir. (1997). *Aqueous Environmental Geochemistry*. New Jersey, prentice- Hall. Inc

Larson, T.E., & Buswell A. M. (1942). Calcium Carbonate Saturation Index and Alkalinity Interpretations. *Journal of American Water Works Association*, 34, 1667

Lê, S., Josse, J., & Husson, F. (2008). FactoMineR: An R Package for Multivariate Analysis. *Journal of Statistical Software*, 25(1), https://doi.org/10.18637/jss.v025.i01.

Lecomte, K.L., Pasquini, A.I., & Depetris, P.J. (2005). Mineral weathering in a semiarid mountain river: Its assessment through PHREEQC inverse modelling. *Aquatic Geochemistry*, 11:173-194.

Li P (2016) Groundwater quality in western China: challenges and paths forward for groundwater

Li, S., Calmels, D., Han, G., Gaillardet, J., & Liu, C. (2008). Sulfuric acid as an agent of carbonate weathering constrained by $\delta^{13}C_{DIC}$: Examples from Southwest China. *Earth and Planetary Science Letters* 270 (2008) 189–199. https://doi.org/10.1016/j.epsl.2008.02.039

Liu, Z.H., Huang, S.B., Sun, G.P., Xu, Z.C., & Xu, M.Y. (2012). Phylogenetic diversity, composition, and distribution of bacterioplankton community in the DongjiangRiver, China. *FEMS Microbiol. Ecol.* 80, 30–44.

Lodder, W. J., van den Berg, H. H. J. L., Rutjes, S. A., & de Roda Husman A. M. (2010). Presence of enteric viruses in source waters for drinking water production in the Netherlands. *Applied and Environmental Microbiology*, 76(17):5965–5971. https://doi.org/10.1128%2FAEM.00245-10

López, M. Isabel; Colomer, Núria; Ruisánchez, Itziar; Callao, M. Pilar (2014). Validation of multivariate screening methodology. Case study: Detection of food fraud. Analytica Chimica Acta, 827(), 28–33. https://doi:10.1016/j.aca.2014.04.019.

Lottermoser, B.G., & Ashley, P.M. (2005). Tailings dam seepage at the rehabilitated Mary Kathleen uranium mine, Australia. *Journal of Geochemical Exploration*, 85; 119-137.

Manoj, K., & Singh, T. N. (2005). Prediction of mine water quality by physical parameters. *Journal of Scientific and Industrial Research*, 64, pp. 564-570, 2005.

Minitab 17 Statistical Software (2010). [Computer software]. *State College, PA: Minitab, Inc.* (www.minitab.com)

Mohan, R., Singh, A.K., Tripathi, J.K., & Chowdhary, G.C. (2000). Hydrochemistry and quality assessment of groundwater in Naini industrial area, Allahabad district, Uttar Pradesh. *Journal of Geological Society of India*, Vol. 55, pp. 77-89, 2000.

Nartey, V. K., Adaboh, R. K., Fianko, J. R., & Donkor, A. (2005). Water quality Assessment of Streams Draining the Akuapim Ridge of Ghana. *West African Journal of Applied Ecology*.8:35-46.

Pallant, J. (2013). SPSS Survival Manual: A Step-by-Step Guide to Data Analysis Using IBM SPSS (5th ed.). New York: McGraw-Hill Education (UK).

Panchani, M.H., Pandya, P.M.J., & Engineering, L.D.C., (2013). Identification and Quantification of Non-Point Sources of pollution to Sabarmati River, Ahmedabad, 75(2), pp.71–75.

Patricia M. Fox; James A. Davis; John M. Zachara (2006). The effect of calcium on aqueous uranium (VI) speciation and adsorption to ferrihydrite and quartz., 70(6), 0–1387. doi: 10.1016/j.gca.2005.11.027

Payne, T. E.; Waite, T. D. (1991). Surface Complexation Modelling of Uranium Sorption Data Obtained by Isotope Exchange Techniques. Radiochimica Acta, 52-53(2), – . doi:10.1524/ract.1991.5253.2.487

Pejman, A. H., Nabi Bidhendi, G. R., Karbassi, A. R., Mehrdadi, N., & Esmaeili Bidhendi, M. (2009). Evaluation of spatial and seasonal variations in surface water quality using multivariate statistical techniques. *Int. J. Environ. Sci. Tech*., Vol. 6, No. 3, pp. 467-476.

Peters, N.E. and Meybeck, M. (2000) Water Quality Degradation Effects on Freshwater Availability: Impacts of Human Activities. Water International, 25, 185-193. https://doi.org/10.1080/02508060008686817.

Phiri, O., Mumba, P., Moyo, B. H. Z., & Kadewa, W. (2005). Assessment of the impact of industrial effluents on water quality of receiving rivers in urban areas of Malawi. *Int. J. Environ. Sci. Tech*., Vol. 2, No. 3, pp. 237-244, 2005.

Plummer, L.N., & Back, W. (1980). The mass balance approach: application to interpreting the chemical evaluation of hydrologic systems. *American Journal of Science*, Vol. 280, pp. 130-142.

Pophare, A. M., & Dewalkar, M. S. (2007). Groundwater quality in Eastern and Southeastern parts of Rajura Tehsil, Chandrapur District, Maharastra. Gond. *Geol. Magz. Spec.* Vol. pp.119-126.

Pradhan, S.K., Patnaik, D., & Rout, S.P. (2001). Ground Water Quality Index for a phosphatic fertilizer plant. *Indian Journal of Environmental Protection.* 21, No.4, pp. 355-358, 2001.

Prassana, M.V. Chidambaram. S.J., & Greech, T.V. (2011). A study on hydrogeochemical characteristics of surface and sub-surface water in and around perumal lake, cuddalore district, Tamil Nadu, South India. *Environment earth sciences*, 63(1), 31-47. Doi.10.,007/s.2665-010-0664-6.

Pu, T. He, Y. Zhang, T., Wu, J., Zhu, G., & Chang, L. (2013). Isotopic and geochemical evolution of ground and river waters in a karst dominated geological setting: a case study from Lijiang basin, South-Asia monsoon region. *Applied Geochemistry*, vol. 33, pp. 199–212.

Qadir, A., Malik, R.N., & Husain, S.Z. (2007). Spatio–temporal variations in water quality of Nullah Aik-tributary of the river Chenab, Pakistan. *Environmental Monitoring and Assessment*, 140, 43–59.

R Core Team (2021). R: A language and environment for statistical computing. R Foundation for Statistical Computing, Vienna, Austria. URL https://www.R-project.org/.

Ramesh, K. (2008). Hydro chemical studies and effect of irrigation on groundwater quality Tondiar basin Tamilnadu. *Unpublished Ph.D thesis, Anna University, Chennai*, Tamilnadu

Ravikumar, P., Somashekar, R. K., & Angami, M. (2011). Hydro chemistry and evaluation of groundwater suitability for irrigation and drinking purposes in the Markandeya River basin, Belgaum District, Karnataka State, *India. Environmental Monitoring and Assessment*, 173(1–4), 459–487. https://doi.org/10. 1007/s10661-010-1399-2

Ray, G E; 1975; The Geology of the Chitipa – Karonga Area Geological Survey of Malawi Bulletin No. 42.

Razmkhah H, Abrishamchi A., & Torkian, A. (2010). Evaluation of spatial and temporal variation in water quality by pattern recognition techniques: a case study on Jajrood River (Tehran, Iran). *J Environ Manag*, 91:852–860.

Rita, N., Kumar, Rajal, S., & Nirmal Kumar, J.I. (2011). An assessment of seasonal variation and water quality index of Sabarmati River and Kharicut canal at Ahmedabad, Gujarat. *Electronic Journal of Environmental, Agricultural and Food Chemistry*, Vol. 10, No. 5, pp. 2248-2261, 2011.

Rodgers Makwinja;Emmanuel Kaunda;Seyoum Mengistou;Tena Alemiew;Friday Njaya;Ishmael Bobby Mphangwe Kosamu;Chikumbusko Chiziwa Kaonga; (2021). Lake Malombe fishing communities' livelihood, vulnerability, and adaptation strategies. Current Research in Environmental Sustainability, (), –. https://doi:10.1016/j.crsust.2021.100055.

Schindler, M., Durocher, J.L., Kotzer, T.G., & Hawthorne, F.C. (2013). Uranium-bearing phases in a U-mill disposal site in Northern Canada: Products of the interaction between leachate/raffinate and tailings material. *Applied Geochemistry*, 29, 151-161.

Schluter, T; 1997 Geology of East Africa Gebruder Borntraeger, Berlin 484pCarter GS, Bennett JD (1973). The geology and mineral resources of Malawi. Bull. Geol. Surv. Malawi 6.

Senthilkumar, K., Nesme,T., Mollier, A., & Pellerin, S. (2012). Regional scale phosphorus flows and budgets within France. The importance of agricultural production systems. *Nutr. Cycl. Agroecosystems*, 92, 145-159. https://doi.org/10.1007/s10705-011-9478-5-5

Shretta & Kazama F. (2007). Assessment of water quality using multivariate statistical techniques. A case study of Fuji-river basis. Japan. *Environmental and modelling software*, 22, 464-475.

Simeonova, P., Simeonov, V., & Andreev, G. (2003). Water quality study of the Struma River Basin, Bulgaria (1989–1998). *Central European Journal of Chemistry 1*, 136–212. aassociation, Jodhpur, pp. 89-98, 1996.

Singh, A.P., & Ghosh, S.K. (1999). Water quality index for River Yamuna. *Poll.Res.*, Vol. 18, pp. 435-439, 1999.

Singh, E.J.K. Gupta, A., & Singh, N.R. (2012). Groundwater quality in Imphal West district, Manipur, India, with multivariate statistical analysis of data. *Environ. Sci. Pollut. Res.*, (1611). Pp.1.

Singh, K. P., Malik, A., Mohan. D., & Sinha, S. (2004). Multivariate statistical techniques for evaluation of spatial and temporal variation on water quality and Gomti River (India)- A case study. *Water Research*, 38, 3980-3992.

Singh, K.P., Malik, A., & Sinha, S., (2005). Water quality assessment and apportionment of pollution sources of Gomti river (India) using multivariate statistical techniques: a case study. *Analytica Chimica Acta*, 538, 355-374.

Singh, R.K., & Choudhary, M.S. (1996). Study of physio-chemical parameters of Groundwater of Nagpur District; some correlation, *28th Annual Convention Issue of Journal of IWWA*, pp.99-102, 1996.

Singh, S.K. (1996). Correlation among different water quality parameters of groundwater of Jhunjhunu District, Rajasthan, *28th Annual Convention of Indian Water Works.*

Smith L., Samways, M., & Taylor P. (2006). Assessing riparian quality using two complementary sets of bio indicators. *Biodiversity Conservation Journal* 16, 2695–2713.

Srinivasamoorthy, K., Chidambaram, S., Prasanna, M. V., Vasanthavihar, M., Peter, J., & Anandhan, P. (2008). Identification of major sources controlling groundwater chemistry from a hard rock terrain - A case study from Mettur taluk, Salem district, Tamil Nadu, India. *Journal of Earth System Science*, 117(1), 49–58. https://doi.org/10.1007/s12040-008-0012-3

Stewart, Brandy D.; Mayes, Melanie A.; Fendorf, Scott (2010). Impact of Uranyl−Calcium−Carbonato Complexes on Uranium (VI) Adsorption to Synthetic and Natural Sediments. Environmental Science & Technology, 44(3), 928–934. https:// doi:10.1021/es902194x.

Stumn, W., & Morgan, J.J. (1996). *Aquatic Chemistry, 2nd edition*. John Wiley, New York, 1981.

Subramani T.J., Rajmohan & Elango, L. 2010). Groundwater geochemistry and identification of hydrogeochemical processes in a hard rock region, southern india. *Environmental monitoring and assessment*, 162(1-4), 123-137. Doi.10.1007/s10661-009-0781-4.

Subramani, T., Elango, L., & Damodarasamy, S. R. (2005). Groundwater quality and its suitability for drinking and agricultural use in Chithar River basin,Tamil Nadu, India. *Journal of Environmental Geology, 47*, 1099–1110. https://doi:10.1007/s00254-005-1243-0

Subramanian, S. (1993). Hydrogeological studies in the coastal aquifer of Tiruchendur, Tamil Nadu, Ph.D Thesis, *Manonmanian Sundaranar University*, *Tirunelveli*, pp. 308, 1994.

Subramanian, V., Hung, M.S., & Hu, M.Y. (1992). An experimental evaluation of neural networks for classification. *Computers and Operations Research*, Vol. 20, pp. 769-782, 1993.

Taiyun, W., & Viliam, S. (2021). R package "corrplot": Visualization of a Correlation Matrix (Version 0.89). https://github.com/taiyun/corrplot

Tiwari, R.N., Dubey, D.P., & Bharti, S.L. (2009). Hydro geochemistry and groundwater quality in Beehar River Basin, Rewa district, Madhya Pradesh, India. *Inter. Jour. Earth Eng. Sci*., v.2(4), pp. 324-330.

Tranter; M. J. Sharp; H. R. Lamb; G. H. Brown; B. P. Hubbard; I. C. Willis (2002). Geochemical weathering at the bed of Haut Glacier d'Arolla, Switzerland—a new model. , 16(5), 959–993. https:// doi:10.1002/hyp.309.

UNEP. (2007). Global Drinking Water Quality Index Development and Sensitivity analysis report. *United Nations environment programme*. Global environment monitoring system/water program.

USEPA (2011). *Edition of the Drinking-Water Standards and Health Advis2ories*. EPA 820–R -11-002. Office of Water, Washington, DC

USEPA. (2009). *Drinking Water Contaminants Guidelines,* Geneva. http://ga.water.usgs.gov/edu/earthgwquality.html

USGS. (2010). *A primer on Water Quality*. Howard Perlman.

USGS. (2014). Contaminants found in groundwater. http//water.usgs.gov/Edu/groundwater-contaminants.html

using isotopic approach ($\delta^{15}N$, $\delta^{18}O$-NO_3 and ^{3}H). *Sci. Total Environ*. 603, 687–698

Varol, M. (2011). Spatial and temporal variations in surface water quality of the dam reservoirs in the Tigris River basin, Turkey. *Catena* 92, 11–21.

Vega M., Pardo., Bardo, E., & Deban, L. (1998). Assessment of seasonal and polluting effects on quality of river water by exploratory data Analysis. *Water research*, 32, 3581-3592.

Wadham, J. L.; Tranter, M.; Skidmore, M.; Hodson, A. J.; Priscu, J.; Lyons, W. B.; Sharp, M.; Wynn, P.; Jackson, M. (2010). Biogeochemical weathering under ice: Size matters. Global Biogeochemical Cycles, 24(3), n/a–n/a. doi: https://10.1029/2009gb003688.

Wang, Aichen; Xie, Lijuan (2014). Technology using near infrared spectroscopic and multivariate analysis to determine the soluble solids content of citrus fruit. Journal of Food Engineering, 143(), 17–24. https://doi:10.1016/j.jfoodeng.2014.06.023.

Wang, J., Da, L., Song, K., & Li, B. (2008). Temporal variations of surface water quality in urban, suburban and rural areas during rapid urbanization in Shanghai, China. *Environ. Pollut*. 152, 387–393.

Wang, Q. (2008). impacts of climate, topography and weathering profile on vadose zone hydrology and coastal pine plantations management-a multi scale investigation, southeast Queensland. *Australia. Bris bone, Queensland University of technology*, PhD Thesis.

Wang, Q., Li, S. Jia, P., & Ding, F. (2013). A review of surface water models. *The Scientific world Journal*.

Ward Jr., J.H. (1963) Hierarchical Grouping to Optimize an Objective Function. Journal of the American Statistical Association, 58, 236-244.

Ward, J.H. (1963). Hierarchical grouping to optimize an objective function. *Journal of the America statistical Association*, 58(301): 236 -244.

Wazne, Mahmoud; Korfiatis, George P.; Meng, Xiaoguang (2003). Carbonate Effects on Hexavalent Uranium Adsorption by Iron Oxyhydroxide. Environmental Science & Technology, 37(16), 3619–3624. https://doi:10.1021/es034166m.

Weaver T.R., & Lawrence C.R. (1999). *Proceedings on Groundwater Sustainable Solution*. University of Melborne, Australia, pp. 637-643.

WHO (1997). *Guideline for drinking water quality*. Health criteria and other supporting informatio, Geneva.

WHO (2004). Guideline for drinking water quality (Addendum). Geneva. Available *@www.who.int/water_sanitationhealth/publications/facts2004/en/index.*

WHO (2011). Guidelines for drinking water quality, WHO(Ed). Retrieved. http://www.who.int/water-sanitation-health/publications/2011/dwq-guildlines/en/

WHO (2011). pH in drinking water @ www.who.int/water-sanitation-health/dwq/ chemicals/ph.pdf. Date accessed: 20-10-2011

WHO/UNICEF/WSSCC. (2004). Things You Need to Know About Sanitation, pp.1–4. Available at: http://www.unwater.org/downloads/media/sanitation/10Things.pdf. Date accessed 12/09/2015.

Wickham, H. (2016). ggplot2: Elegant Graphics for Data Analysis. Springer-Verlag, New York.

Wilde, A, Corbin J.C., Mwenelupembe, J., Princep, D., Otto, A., & Becker, E. (2019). Geology of the Kayelekera uranium deposit, Malawi. *IAEA 2019 UPC selected papers 2012-2015, Proceedings of a Series of Technical Meetings*, IAEA TECDOC-1873. IAEA

Wu,Y., Li, J., Wang, Y., & Xie, X. (2018). Variations of uranium concentrations in a multi-aquifer system under the impact of surface water-groundwater interaction, *Journal of Contaminant Hydrology*, 211: 65-76. https://doi.org/10.1016/j.jconhyd.2018.03.007

Xu, H. Hou, Z., Liu, X. & Dong, J. (2010). Major ion chemistry of waters in Lake Qinghai catchments, NE Qinghai- Tibet plateau, China, *Quaternary International*, vol. 212, no. 1, pp. 35–43, 2010.

Xu, Z., & Liu, C-Q. (2007) Chemical weathering in the upper reaches of Xijiang River draining the Yunnan–Guizhou Plateau, Southwest China. *Chemical Geology*. 239 83–95.

Yidana, S.M. (2010). Groundwater classification using multivariate statistical methods, southern Ghana. *Journal Africa earth Sciences*, 57(5) -455-469. http: //dx.doi.org/10.1016/j.j.afrearsci.2009.12-002

Zhang, Y., Jiang, Y., Yuana, D., Cui, J., Li, Y., Yang, J., & Cao, M. (2020). Source and flux of anthropogenically enhanced dissolved inorganic carbon: A comparative study of urban and forest karst catchments in Southwest China. *Science of the Total Environment* 138255. https://doi.org/10.1016/j.scitotenv.2020.138255

Zhang, Z. Tan. X, Li. S., & Bu. H. (2010). Surface water quality and its control in a river with intensive human impacts--a case study of the Xiangjiang River, China. *Journal of environmental management*, 91(12), 2483–90.

Zhao, Z., Liu, G., Liu, Q., Huang, C., & Li, H. (2018). Studies on the Spatiotemporal Variability of River Water Quality and Its Relationships with Soil and Precipitation: A Case Study of the Mun River Basin in Thailand. *Int. J. Environ. Res. Public Health*, 15, 2466.

Zhou, F., Huang, G.H., Guo, H.C., Zhang, W., & Hao, Z.J. (2007). Spatio-temporal patterns and source apportionment of coastal water pollution in eastern Hong Kong. *Water Res*. 41, 3429–3439.

LIST OF APPENDICES

3.5 Appendix 1: Summary of physio-chemical characteristics of surface water in the study area

CODE	EC (µS/cm)		TDS (ppm)		Water Temperature (ºC)		DO (mg/L)		ORP (mV)	
	WTS	DRS	WTS	DRS	WTS	DRS	WTS	DRS	WTS	DRS
S01	205.0	234.00	146.00	146.00	25.07	25.07	7.12	7.23	132	121.00
S02	165.8	180.00	117.80	125.00	25.00	25.00	6.98	7.12	150	150.00
S03	139.1	150.10	98.89	102.00	25.34	25.34	6.89	6.80	138	139.00
S04	206.0	130.20	179.50	120.00	26.10	26.70	7.30	7.20	150	123.00
S05	142.1	122.30	101.10	158.00	25.87	27.00	7.02	5.99	116	94.89
S06	144.1	175.00	101.00	120.00	26.00	26.00	7.42	7.56	150	135.00
S07	155.4	170.00	109.08	112.00	25.09	25.09	7.00	7.09	156	144.00
S08	155.4	160.20	110.10	120.10	26.07	26.07	7.23	7.42	118	150.00
S09	138.4	254.00	98.10	181.00	25.32	26.90	7.08	6.00	118	99.60
S10	279.0	300.20	198.00	210.00	26.00	25.40	7.40	7.43	145	140.00
S11	160.0	216.00	138.10	108.00	25.32	25.00	8.06	6.19	114	114.70
S12	154.6	209.00	109.70	109.00	24.82	26.00	6.73	6.11	144	108.90
S13	309.0	210.00	260.79	105.00	24.51	25.78	7.11	6.34	154	118.00
S14	210.1	223.00	156.00	112.00	25.00	27.00	7.25	6.24	137	121.30

S15	97.8	130.00	69.10	115.00	26.74	26.76	7.04	6.39	132	88.90
S16	60.1	67.00	50.45	50.00	26.90	26.09	7.06	7.10	122	93.90
S17	98.0	53.00	74.00	27.00	25.25	27.30	6.42	5.97	148	98.50
S18	64.9	108.90	46.10	98.00	26.74	25.08	6.84	6.98	151	108.90
S19	54.0	166.00	33.80	118.00	28.11	27.00	7.12	6.35	155	104.40

Concentration values: **S**: sampling point. **WTS**: wet season. **DYS:** dry season

	pH		**HCO_3^- (mg/L)**		**SO_4^{2-} (mg/L)**		**NO_3^- (mg/L)**		**Cl^- (mg/L)**		**Ca (mg/L)**	
CODE	**WTS**	**DRS**	**WTS**	**DRS**	**WTS**	**DRS**	**WTS**	**DRS**	**WTS**	**DRS**	**WTS**	**DRS**
S01	8.10	7.90	54	50.00	1.23	5.78	1.45	2.45	14.67	15.32	9.03	8.09
S02	7.89	8.00	70	65.00	1.45	2.01	2.00	2.20	6.75	7.01	12.90	9.07
S03	8.32	8.23	67	58.00	5.68	3.90	1.90	2.70	7.64	7.80	9.90	11.78
S04	8.45	8.40	66	55.00	7.60	4.90	2.81	3.20	10.67	13.60	7.31	10.09
S05	8.52	8.40	58	56.00	6.09	6.90	0.00	1.68	7.32	8.98	8.34	10.78
S06	8.38	8.23	58	45.00	4.16	3.44	2.02	2.05	13.90	14.01	8.02	8.88
S07	7.94	7.96	75	70.00	2.34	1.02	0.22	0.31	8.97	9.21	10.23	11.34
S08	8.00	8.06	76	80.00	1.98	0.98	0.22	0.28	7.11	7.32	11.34	11.50
S09	8.51	8.58	51	50.00	4.80	7.32	4.80	1.89	3.98	10.47	10.80	7.34
S10	7.28	7.79	105	100.00	15.00	16.23	1.30	1.50	9.08	8.90	14.30	16.78
S11	8.24	8.65	72	60.00	5.89	13.20	0.00	1.97	13.86	19.80	10.60	19.09
S12	8.40	8.69	62	50.20	30.31	12.50	0.12	1.43	10.60	16.00	14.06	17.50

S13	8.42	8.83	78	70.00	72.00	22.60	0.68	1.95	4.67	14.05	18.98	21.30
S14	8.32	8.40	64	82.00	65.23	18.90	1.58	1.86	8.80	17.60	15.06	23.60
S15	8.61	8.09	40	33.00	5.40	6.98	0.00	3.08	5.04	24.00	5.08	10.89
S16	8.18	8.26	25	23.00	4.80	5.20	2.99	1.28	5.04	16.09	4.20	6.49
S17	8.01	8.10	40	24.00	8.00	12.88	1.26	2.19	7.23	7.98	4.56	6.78
S18	8.09	8.33	37	40.00	4.45	2.08	4.00	2.56	7.79	19.00	5.67	10.57
S19	7.99	8.04	25	32.00	6.80	2.25	9.02	3.40	10.45	27.40	7.67	12.08

Concentration values: **S**: sampling point. **WTS**: wet season. **DYS:** dry season

	Mg (mg/L)		**K (mg/L)**		**Na (mg/L)**		**Fe (mg/L)**		**U (mg/L)**		**Si (mg/L)**	
CODE	**WTS**	**DRS**	**WTS**	**DRS**	**WTS**	**DRS**	**WTS**	**DRS**	**WTS**	**DRS**	**WTS**	**DRS**
S01	3.98	8.73	2.41	2.50	5.50	5.50	0.01	0.01	0.006	0.004	4.04	4.00
S02	4.12	8.20	3.25	3.33	3.42	3.42	0.02	0.01	0.000	0.000	4.60	4.70
S03	5.55	6.03	1.52	1.60	3.32	3.32	0.00	0.00	0.000	0.000	4.78	4.72
S04	4.80	8.73	2.92	3.12	4.31	5.31	0.01	0.00	0.000	0.000	5.20	5.23
S05	4.10	5.46	4.09	2.34	3.21	10.17	0.00	0.00	0.002	0.003	4.78	4.98
S06	5.70	5.80	5.32	5.44	5.00	7.00	0.01	0.00	0.001	0.000	5.44	5.60
S07	5.37	5.65	3.37	3.35	8.88	8.88	0.00	0.01	0.000	0.000	5.06	5.04
S08	5.62	5.60	2.49	2.70	6.90	6.90	0.00	0.00	0.000	0.000	6.01	6.11
S09	4.56	5.50	3.98	2.28	4.06	9.75	0.01	0.00	0.002	0.004	5.17	5.07

S10	7.54	9.02	2.43	2.48	10.90	10.90	0.01	0.01	0.001	0.001	4.31	4.50
S11	6.43	5.20	2.79	2.85	6.89	12.89	0.01	0.01	0.004	0.007	4.12	4.20
S12	6.90	4.00	2.89	3.02	7.09	10.02	0.02	0.01	0.005	0.007	5.23	7.13
S13	6.82	8.23	5.20	2.96	7.98	10.92	0.04	0.01	0.005	0.005	4.10	4.30
S14	7.10	7.23	4.88	2.93	7.80	14.34	0.05	0.01	0.004	0.003	5.56	5.46
S15	3.88	5.89	2.72	2.76	6.89	6.60	0.02	0.00	0.005	0.007	3.11	3.23
S16	1.75	2.20	1.10	1.18	2.56	3.70	0.28	0.00	0.008	0.009	3.73	3.45
S17	1.86	2.00	2.44	2.48	3.80	4.48	0.05	0.01	0.001	0.002	4.17	4.37
S18	1.15	2.64	3.10	1.30	3.45	5.40	0.18	0.00	0.008	0.007	4.12	4.11
S19	2.87	2.98	1.86	1.43	2.89	6.59	0.04	0.00	0.001	0.001	4.21	4.29

Concentration values: **S**: sampling point. **WTS**: wet season. **DYS:** dry season